Electronic Supplementary Information for

CO_2 fixation and transformation on a thiolate-bridged dicobalt scaffold under oxidising conditions

Hui Wu,[a] Jianzhe Li,[a] Dawei Yang*[a], Peng Tong,[a] Jinfeng Zhao,[a] Baomin Wang[a] and Jingping Qu*[ab]

[a]*State Key Laboratory of Fine Chemicals, Dalian University of Technology, Dalian 116024, P. R. China*

[b]*Key Laboratory for Advanced Materials, East China University of Science and Technology, Shanghai 200237, P. R. China*

*E-mail: qujp@dlut.edu.cn

yangdw@dlut.edu.cn

Table of Contents

I. X-ray Crystallographic Data

Table S1. Crystallographic data for **1** and **2**

	1	**2**
Formula	$C_{24}H_{40}Co_2S_2$	$C_{25}H_{40}Co_2O_3S_2$
Formula weight	510.54	570.55
Crystal dimensions (mm^3)	0.30 × 0.24 × 0.20	0.28 × 0.24 × 0.21
Crystal system	Monoclinic	Monoclinic
Space group	P 21/m	C 2/c
a (Å)	8.0243(7)	18.7475(6)
b (Å)	15.9984(13)	12.8019(4)
c (Å)	10.5134(9)	10.6678(3)
α (°)	90. 00	90.00
β (°)	111.481(2)	93.1660(10)
γ (°)	90.00	90.00
Volume ($Å^3$)	1255.92(19)	2556.40(14)
Z	2	4
T (K)	223(2)	173(2)
D_{calcd} ($g\ cm^{-3}$)	1.350	1.482
μ (mm^{-1})	1.495	1.486
F (000)	540	1200
No. of rflns. collected	15786	24564
No. of indep. rflns. /R_{int}	2300 / 0.0543	2253 / 0.0262
No. of obsd. rflns. [$I_0 > 2\sigma(I_0)$]	2031	2112
Data / restraints / parameters	2300 / 66 / 165	2253 / 0 / 146
R_1 / wR_2 [$I_0 > 2\sigma(I_0)$]	0.0486 / 0.1310	0.0315 / 0.0945
R_1 / wR_2 (all data)	0.0559 / 0.1338	0.0334 / 0.0957
GOF (on F^2)	1.190	1.064
Largest diff. peak and hole (e $Å^{-3}$)	0.562 / −0.715	0.499 / −0.469
CCDC No.	1904424	1904422

Table S2. Crystallographic data for **3[BF_4]** and **4[BF_4]**

	3[BF_4]	**4[BF_4]**
Formula	$C_{25}H_{41}BCo_2F_4O_3S_2$	$C_{26}H_{43}BCo_2F_4O_3S_2$
Formula weight	658.37	672.39
Crystal dimensions (mm^3)	0.32 × 0.26 × 0.24	0.32 × 0.26 × 0.20
Crystal system	Triclinic	Monoclinic
Space group	P −1	P 21/n
a (Å)	8.5950(5)	8.4551(6)
b (Å)	11.9610(7)	13.8353(11)
c (Å)	14.2279(8)	25.1199(19)
α (°)	76.4760(10)	90.00
β (°)	86.4300(10)	96.7756(16)
γ (°)	88.2390(10)	90.00
Volume ($Å^3$)	1419.18(14)	2918.0(4)
Z	2	4
T (K)	173(2)	173(2)
D_{calcd} (g cm^{-3})	1.541	1.531
μ (mm^{-1})	1.368	1.332
F (000)	684	1400
No. of rflns. collected	31858	63745
No. of indep. rflns. /R_{int}	4965 / 0.0203	5127 / 0.0410
No. of obsd. rflns. [$I_0 > 2\sigma(I_0)$]	4763	4733
Data / restraints / parameters	4965 / 0 / 334	5127 / 1249 / 343
R_1 / wR_2 [$I_0 > 2\sigma(I_0)$]	0.0330 / 0.0959	0.0536 / 0.1375
R_1 / wR_2 (all data)	0.0344 / 0.0968	0.0578 / 0.1401
GOF (on F^2)	1.040	1.026
Largest diff. peak and hole (e $Å^{-3}$)	0.618 / −0.593	1.369 / −1.552
CCDC No.	1904423	1904417

Table S3. Crystallographic data for **5a[PF_6]** and **5b[PF_6]**

	5a[PF_6]	**5b[PF_6]**
Formula	$C_{26}H_{43}Co_2F_6O_3PS_2$	$C_{27}H_{45}Co_2F_6O_3PS_2$
Formula weight	730.55	744.58
Crystal dimensions (mm^3)	0.28 × 0.24 × 0.20	0.29 × 0.27 × 0.22
Crystal system	Monoclinic	Monoclinic
Space group	P 21/c	P 21/c
a (Å)	8.5889(4)	8.6079(6)
b (Å)	14.0677(7)	14.3633(10)
c (Å)	25.9890(12)	25.9474(19)
α (°)	90.00	90.00
β (°)	98.0250(10)	96.4298(14)
γ (°)	90.00	90.00
Volume ($Å^3$)	3109.4(3)	3187.9(4)
Z	4	4
T (K)	243(2)	190(2)
D_{calcd} (g cm^{-3})	1.561	1.551
μ (mm^{-1})	1.316	1.285
F (000)	1512	1544
No. of rflns. collected	31638	31471
No. of indep. rflns. /R_{int}	5478 / 0.1048	5577 / 0.0240
No. of obsd. rflns. [$I_0 > 2\sigma(I_0)$]	3941	5321
Data / restraints / parameters	5478 / 0 / 361	5577 / 0 / 370
R_1 / wR_2 [$I_0 > 2\sigma(I_0)$]	0.0623 / 0.1328	0.0417 / 0.1128
R_1 / wR_2 (all data)	0.0971 / 0.1441	0.0434 / 0.1137
GOF (on F^2)	1.043	1.063
Largest diff. peak and hole (e $Å^{-3}$)	0.782 / −0.392	0.609 / −0.448
CCDC No.	1904418	1904425

Table S4. Crystallographic data for **6a[PF_6]**, **6b[PF_6]** and **6c[PF_6]**

	6a[PF_6]	**6b[PF_6]**	**6c[PF_6]**
Formula	$C_{29}H_{50}Co_2F_6NO_2PS_2$	$C_{28}H_{47}Co_2F_6NO_2PS_2$	$C_{29}H_{50}Co_2F_6NO_2PS_2$
Formula weight	771.65	756.61	771.65
Crystal dimensions (mm^3)	0.32 × 0.25 × 0.21	0.32 × 0.28 × 0.26	0.33 × 0.27 × 0.23
Crystal system	Monoclinic	Monoclinic	Monoclinic
Space group	P 21/c	P 21/n	C 2/c
a (Å)	16.2996(10)	15.3556(9)	20.2675(9)
b (Å)	8.8769(5)	11.3607(6)	11.2385(5)
c (Å)	24.0942(14)	20.2644(11)	15.4741(7)
α (°)	90.00	90.00	90.00
β (°)	94.1780(10)	108.5488(10)	104.8430(10)
γ (°)	90.00	90.00	90.00
Volume ($Å^3$)	3476.9(4)	3351.5(3)	3407.0(3)
Z	4	4	4
T (K)	173(2)	173(2)	173(2)
D_{calcd} (g cm^{-3})	1.474	1.499	1.504
μ (mm^{-1})	1.179	1.222	1.204
F (000)	1608	1572	1608
No. of rflns. collected	32446	43759	21048
No. of indep. rflns. /R_{int}	6039/ 0.0178	5864 / 0.0246	2996 / 0.0245
No. of obsd. rflns. [$I_0 > 2\sigma(I_0)$]	5851	5469	2864
Data / restraints / parameters	6039 / 0 / 388	5864 / 0 / 379	2996 / 0 / 197
R_1 / wR_2 [$I_0 > 2\sigma(I_0)$]	0.0450 / 0.1228	0.0379 / 0.1083	0.0414 / 0.1195
R_1 / wR_2 (all data)	0.0460 / 0.1235	0.0405 / 0.1102	0.0431 / 0.1210
GOF (on F^2)	1.057	0.988	1.035
Largest diff. peak and hole (e $Å^{-3}$)	1.139 / −0.689	0.649 / −0.578	1.087 / −0.585
CCDC No.	1904421	1904420	1904419

Fig. S1. ORTEP diagram of **1**

The thermal ellipsoids are shown at 50% probability level. Hydrogen atoms are omitted for clarity.

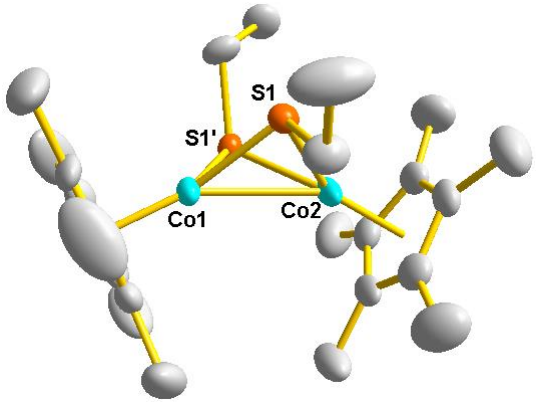

Table S5. Selected bond distances (Å) and angles (°) for **1**

Distances (Å)			
Co1–Co2	2.5472(10)		
Co1–S1	2.140(2)	Co1–S1'	2.303(2)
Co2–S1	2.090(2)	Co2–S1'	2.364(2)
Co1–Cp*1	1.7117(8)	Co2–Cp*2	1.6913(7)
Angles (°)			
Co1–S1–Co2	74.04(7)	Co1–S1'–Co2	66.14(6)
Torsion angles (°)			
S1–Co1Co2–S1'	109.91(10)	S1'–Co1Co2–S1	109.91(10)
Dihedral angles (°)			
Cp*1–Cp*2	54.04(18)		

Fig. S2. ORTEP diagram of **2**

The thermal ellipsoids are shown at 50% probability level. Hydrogen atoms are omitted for clarity.

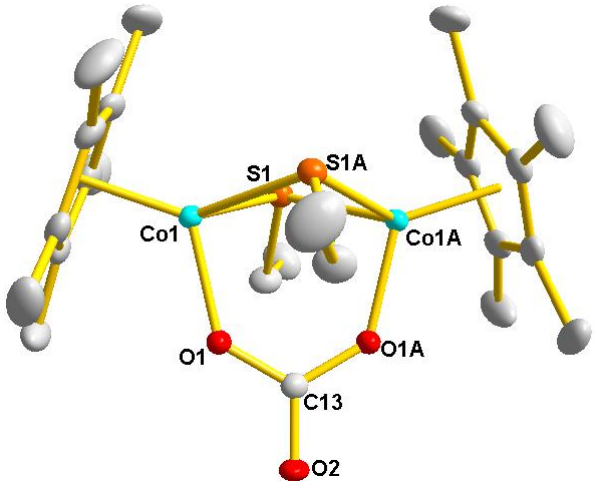

Table S6. Selected bond distances (Å) and angles (°) for **2**

Distances (Å)			
Co1···Co1A	3.1535(1)		
Co1–S1	2.2293(7)	Co1–O1	1.9167(17)
O1–C13	1.311(2)	C13–O2	1.243(4)
Co1–Cp*1	1.6954(3)		
Angles (°)			
Co1–S1–Co1A	89.83(2)	Co1–O1–C13	132.50(17)
O1–C13–O2	119.44(15)	O1–C13–O1A	121.1(3)
Torsion angles (°)			
S1–Co1Co2–S1A	142.044(35)		
Dihedral angles (°)			
Cp*1–Cp*2	37.95(12)		

Fig. S3. ORTEP diagram of **3[BF_4]**

The thermal ellipsoids are shown at 50% probability level. Hydrogen atoms on carbons and counter anion BF_4^- are omitted for clarity.

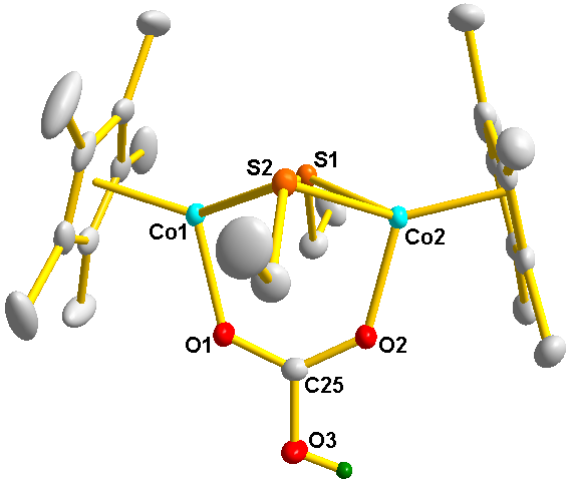

Table S7. Selected bond distances (Å) and angles (°) for **3[BF_4]**

Distances (Å)			
Co1···Co2	3.1966(5)	Co1–S1	2.2530(7)
Co1–S2	2.2543(7)	Co2–S1	2.2521(7)
Co2–S2	2.2497(7)	Co1–O1	1.9624(18)
Co2–O2	1.9448(17)	O1–C25	1.257(3)
O2–C25	1.254(3)	O3–C25	1.340(3)
Co1–Cp*1	1.6873(4)	Co2–Cp*2	1.6831(3)
Angles (°)			
Co1–S1–Co2	90.40(2)	Co1–S2–Co2	90.43(2)
Co1–O1–C25	128.55(16)	Co2–O2–C25	130.69(16)
O1–C25–O2	128.4(2)	O1–C25–O3	115.0(2)
O2–C25–O3	116.5(2)		
Torsion angles (°)			
S1–Co1Co2–S2	137.544(34)		
Dihedral angles (°)			
Cp*1–Cp*2	33.213(97)		

Fig. S4. ORTEP diagram of **4[BF_4]**

The thermal ellipsoids are shown at 50% probability level. Hydrogen atoms and counter anion BF_4^- are omitted for clarity.

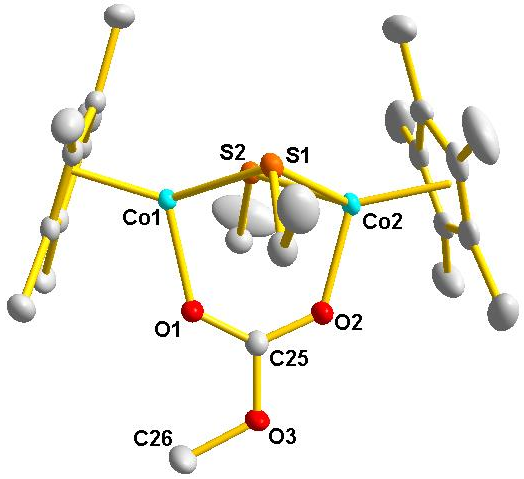

Table S8. Selected bond distances (Å) and angles (°) for **4[BF_4]**

Distances (Å)			
Co1···Co2	3.1942(8)		
Co1–S1	2.2499(11)	Co1–S2	2.2419(11)
Co2–S1	2.2564(11)	Co2–S2	2.2463(12)
Co1–O1	1.956(3)	Co2–O2	1.958(3)
O1–C25	1.253(5)	O2–C25	1.250(5)
O3–C25	1.342(5)	O3–C26	1.453(6)
Co1–Cp*1	1.6807(6)	Co2–Cp*2	1.7147(5)
Angles (°)			
Co1–S1–Co2	90.28(4)	Co1–S2–Co2	90.75(4)
Co2–O2–C25	129.1(3)	Co1–O1–C25	129.7(3)
O1–C25–O2	128.8(4)	O2–C25–O3	113.6(4)
O1–C25–O3	117.6(4)	C25–O3–C26	117.5(3)
Torsion angles (°)			
S3–Co1Co2–S4	138.738(59)		
Dihedral angles (°)			
Cp*1–Cp*2	35.08(20)		

Fig. S5. ORTEP diagram of **5a[PF_6]**

The thermal ellipsoids are shown at 50% probability level. Hydrogen atoms and counter anion PF_6^- are omitted for clarity.

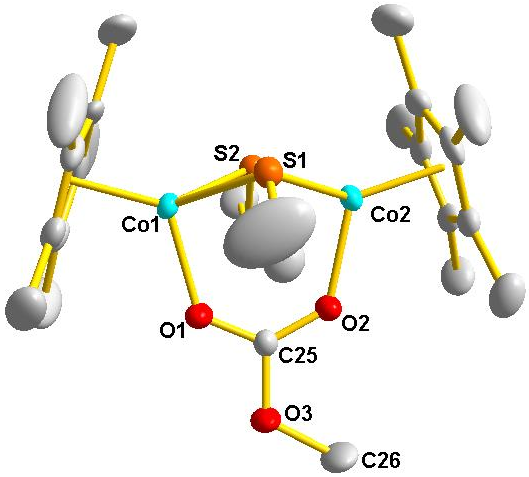

Table S9. Selected bond distances (Å) and angles (°) for **5a[PF_6]**

Distances (Å)			
Co1···Co2	3.1814(10)		
Co1–S1	2.2410(15)	Co1–S2	2.2535(15)
Co2–S1	2.2428(15)	Co2–S2	2.2443(15)
Co1–O1	1.972(3)	Co2–O2	1.966(3)
O1–C25	1.258(6)	O2–C25	1.247(6)
O3–C25	1.338(6)	O3–C26	1.449(7)
Co1–Cp*1	1.6932(7)	Co2–Cp*2	1.6819(7)
Angles (°)			
Co1–S1–Co2	90.38(5)	Co1–S2–Co2	90.02(5)
Co2–O2–C25	129.7(3)	Co1–O1–C25	128.6(3)
O1–C25–O2	128.8(5)	O2–C25–O3	118.5(4)
O1–C25–O3	112.7(4)	C25–O3–C26	117.4(4)
Torsion angles (°)			
S1–Co1Co2–S2	139.143(75)		
Dihedral angles (°)			
Cp*1–Cp*2	35.64(20)		

Fig. S6. ORTEP diagram of **5b[PF_6]**

The thermal ellipsoids are shown at 50% probability level. Hydrogen atoms and counter anion PF_6^- are omitted for clarity.

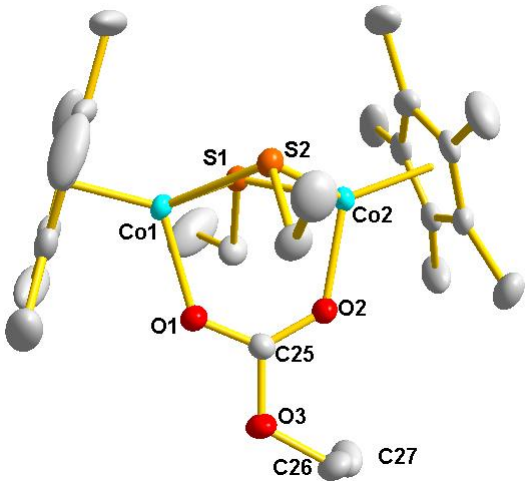

Table S10. Selected bond distances (Å) and angles (°) for **5b[PF_6]**

Distances (Å)			
Co1···Co2	3.1851(7)	Co1–S1	2.2517(9)
Co1–S2	2.2419(9)	Co2–S1	2.2611(9)
Co2–S2	2.2459(9)	Co1–O1	1.969(2)
Co2–O2	1.957(2)	O1–C25	1.257(4)
O2–C25	1.258(4)	O3–C25	1.341(4)
O3–C26	1.458(4)	C26–C27	1.490(6)
Co1–Cp*1	1.6866(4)	Co2–Cp*2	1.6875(5)
Angles (°)			
Co1–S1–Co2	89.78(3)	Co1–S2–Co2	90.42(3)
Co1–O1–C25	129.1(2)	Co2–O2–C25	129.4(2)
O1–C25–O2	128.5(3)	O1–C25–O3	119.1(3)
O2–C25–O3	112.3(3)	C25–O3–C26	118.4(3)
Torsion angles (°)			
S3–Co1Co2–S4	139.869(45)		
Dihedral angles (°)			
Cp*1–Cp*2	36.42(12)		

Fig. S7. ORTEP diagram of **6a[PF_6]**

The thermal ellipsoids are shown at 50% probability level. Hydrogen atoms on carbons and counter anion PF_6^- are omitted for clarity.

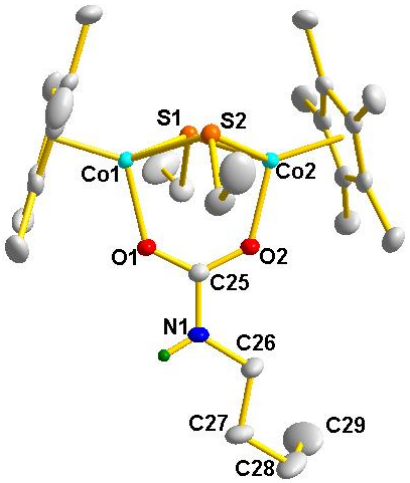

Table S11. Selected bond distances (Å) and angles (°) for **6a[PF_6]**

Distances (Å)			
Co1···Co2	3.1725(6)	Co1–S1	2.2424(8)
Co1–S2	2.2470(8)	Co2–S1	2.2458(8)
Co2–S2	2.2476(8)	Co1–O1	1.940(2)
Co2–O2	1.946(2)	O1–C25	1.272(4)
O2–C25	1.266(4)	N1–C25	1.356(4)
N1–C26	1.456(4)	C26–C27	1.515(5)
Co1–Cp*1	1.6871(4)	Co2–Cp*2	1.6835(5)
Angles (°)			
Co1–S1–Co2	89.96(3)	Co1–S2–Co2	89.80(3)
Co1–O1–C25	129.8(2)	Co2–O2–C25	129.6(2)
O1–C25–O2	127.3(3)	O1–C25–N1	116.3(3)
O2–C25–N1	116.4(3)	C25–N1–C26	122.0(3)
Torsion angles (°)			
S1–Co1Co2–S2	139.144(40)		
Dihedral angles (°)			
Cp*1–Cp*2	36.614(115)		

Fig. S8. ORTEP diagram of **6b[PF_6]**

The thermal ellipsoids are shown at 50% probability level. Hydrogen atoms on carbons and counter anion PF_6^- are omitted for clarity.

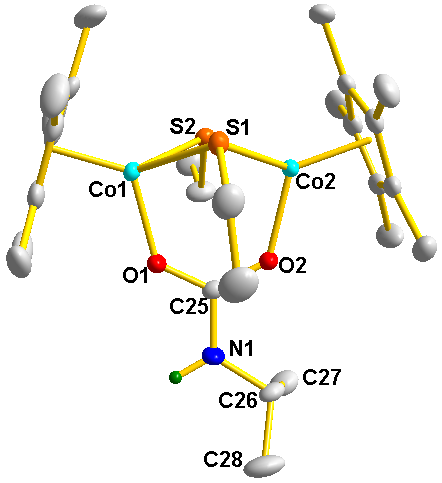

Table S12. Selected bond distances (Å) and angles (°) for **6b[PF_6]**

Distances (Å)			
Co1···Co2	3.1939(5)	Co1–S1	2.2264(7)
Co1–S2	2.2602(7)	Co2–S1	2.2327(7)
Co2–S2	2.2576(7)	Co1–O1	1.9417(19)
Co2–O2	1.9460(18)	O1–C25	1.274(3)
O2–C25	1.270(3)	N1–C25	1.356(3)
N1–C26	1.461(4)	C26–C27	1.518(4)
Co1–Cp*1	1.6853(3)	Co2–Cp*2	1.6875(3)
Angles (°)			
Co1–S1–Co2	91.49(3)	Co1–S2–Co2	89.97(3)
Co1–O1–C25	130.23(17)	Co2–O2–C25	129.75(16)
O1–C25–O2	127.1(2)	O1–C25–N1	115.7(2)
O2–C25–N1	117.2(2)	C25–N1–C26	123.2(2)
Torsion angles (°)			
S1–Co1Co2–S2	135.73(4)		
Dihedral angles (°)			
Cp*1–Cp*2	38.1(1)		

Fig. S9. ORTEP diagram of **6c[PF_6]**

The thermal ellipsoids are shown at 50% probability level. Hydrogen atoms on carbons and counter anion PF_6^- are omitted for clarity.

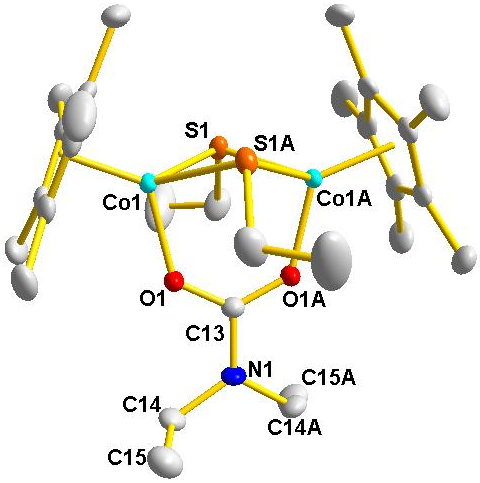

Table S13. Selected bond distances (Å) and angles (°) for **6c[PF_6]**

Distances (Å)			
Co1···Co1A	3.1842(1)		
Co1–S1	2.2397(8)	Co1–O1	1.939(2)
O1–C13	1.274(3)	C13–N1	1.354(5)
N1–C14	1.447(4)	C14–C15	1.510(5)
Co1–Cp*1	1.6956(1)		
Angles (°)			
Co1–S1–Co1A	90.50(3)	Co1–O1–C13	130.0(2)
O1–C13–N1	116.54(19)	C13–N1–C14	120.99(18)
O1–C13–O1A	126.9(4)	C14–N1–C14A	118.0(4)
Torsion angles (°)			
S1–Co1Co1A–S1A	140.379(2)		
Dihedral angles (°)			
Cp*1–Cp*2	44.234		

II. NMR Spectra

Fig. S10. ^{1}H NMR spectrum of **1** in $CDCl_3$

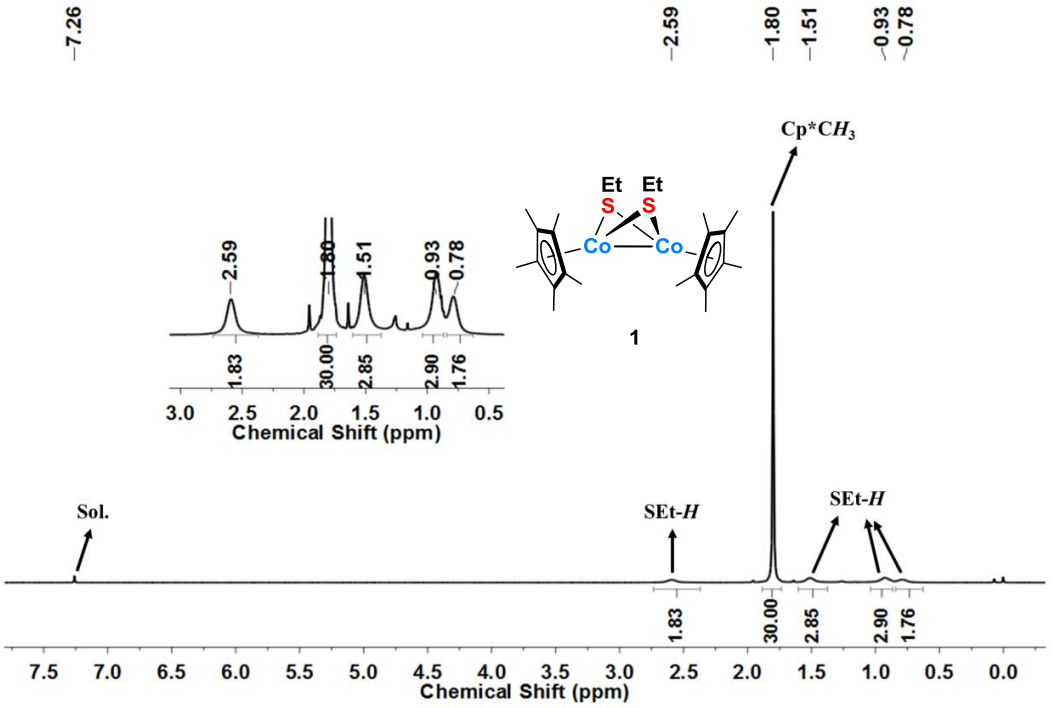

Fig. S11. ^{13}C NMR spectrum of **1** in $CDCl_3$

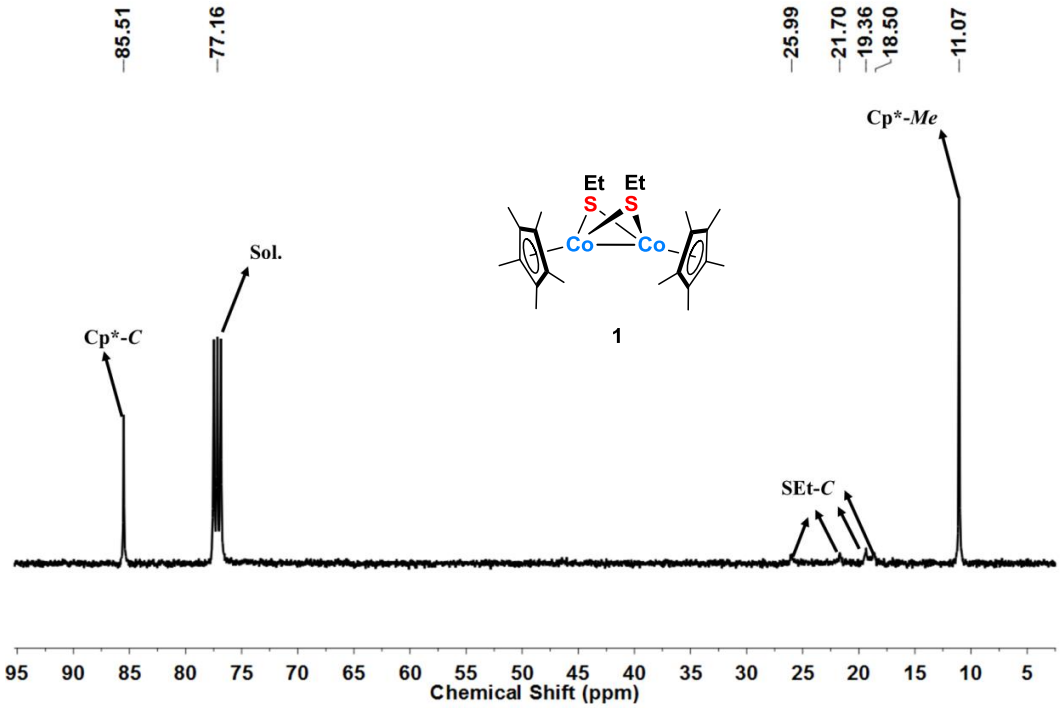

Fig. S12. ^{1}H NMR spectrum of **2** in $CDCl_3$

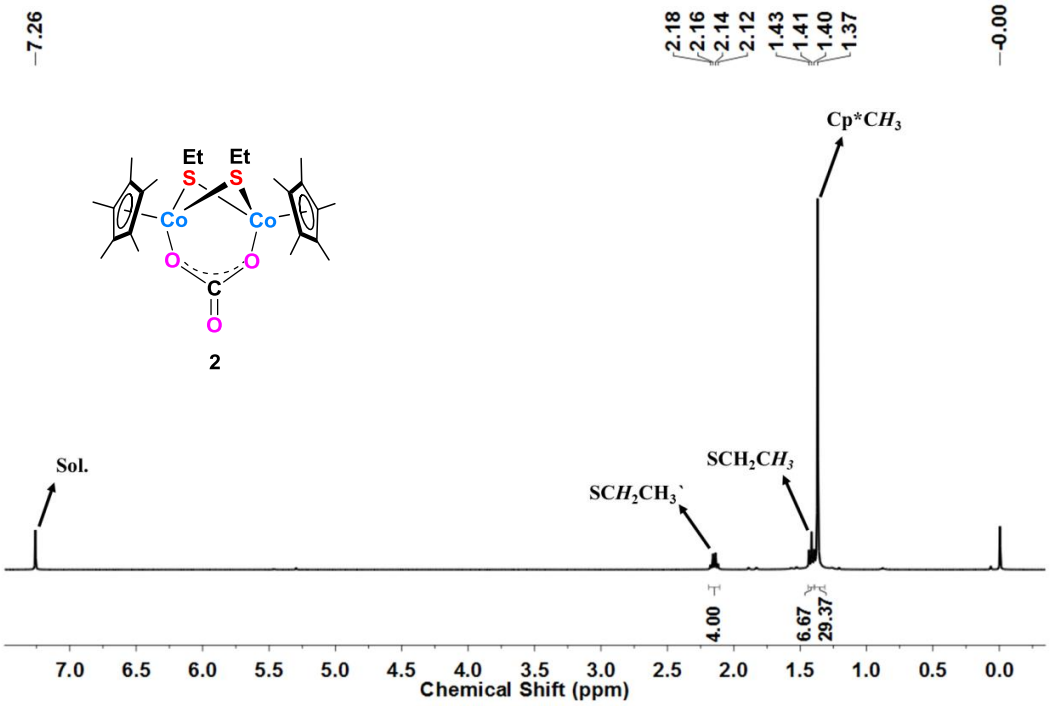

Fig. S13. ^{13}C NMR spectrum of **2** in $CDCl_3$

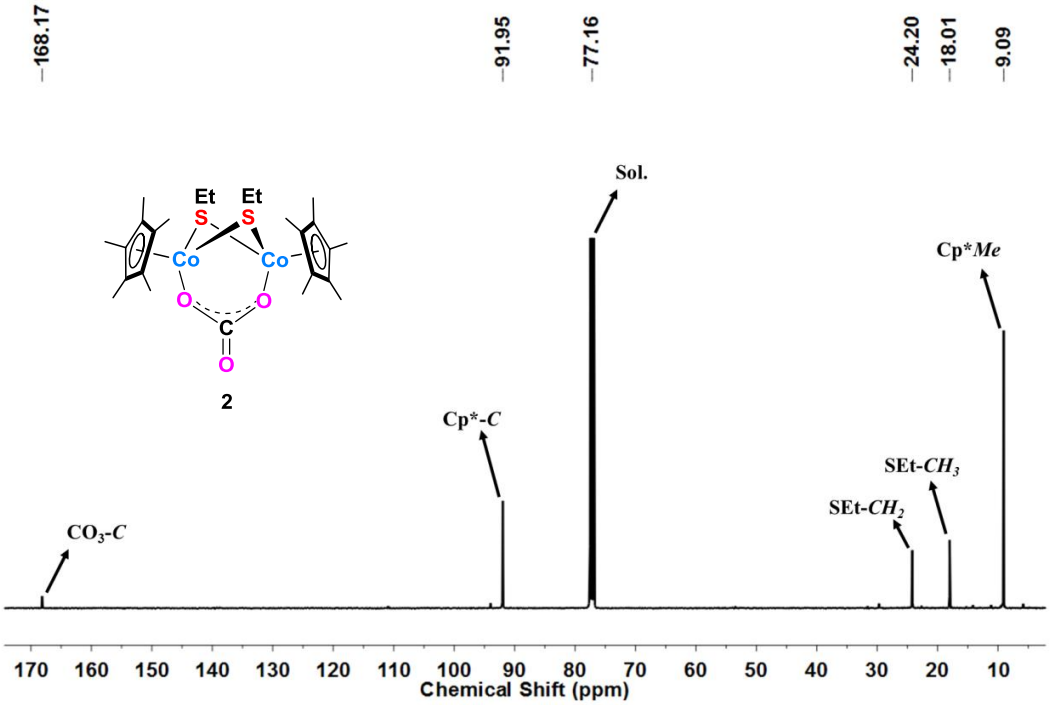

Fig. S14. ^{1}H NMR spectrum of **3[BF$_4$]** in CD_2Cl_2

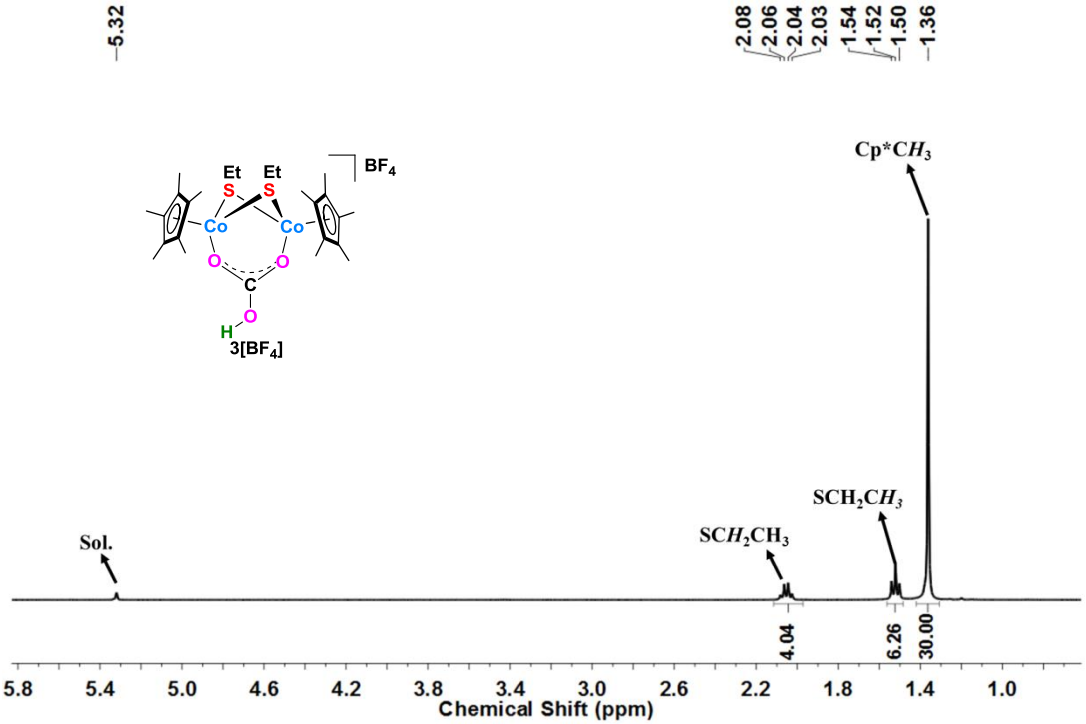

Fig. S15. ^{13}C NMR spectrum of **3[BF$_4$]** in CD_2Cl_2

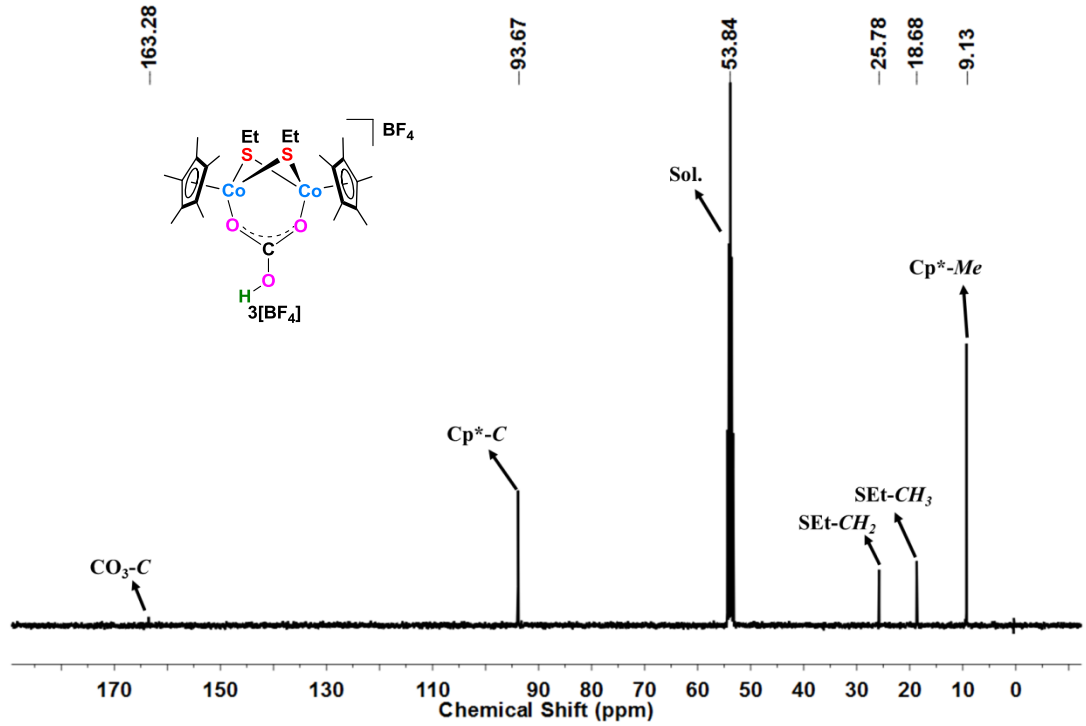

Fig. S16. ^{19}F NMR spectrum of **3[BF$_4$]** in CD_2Cl_2

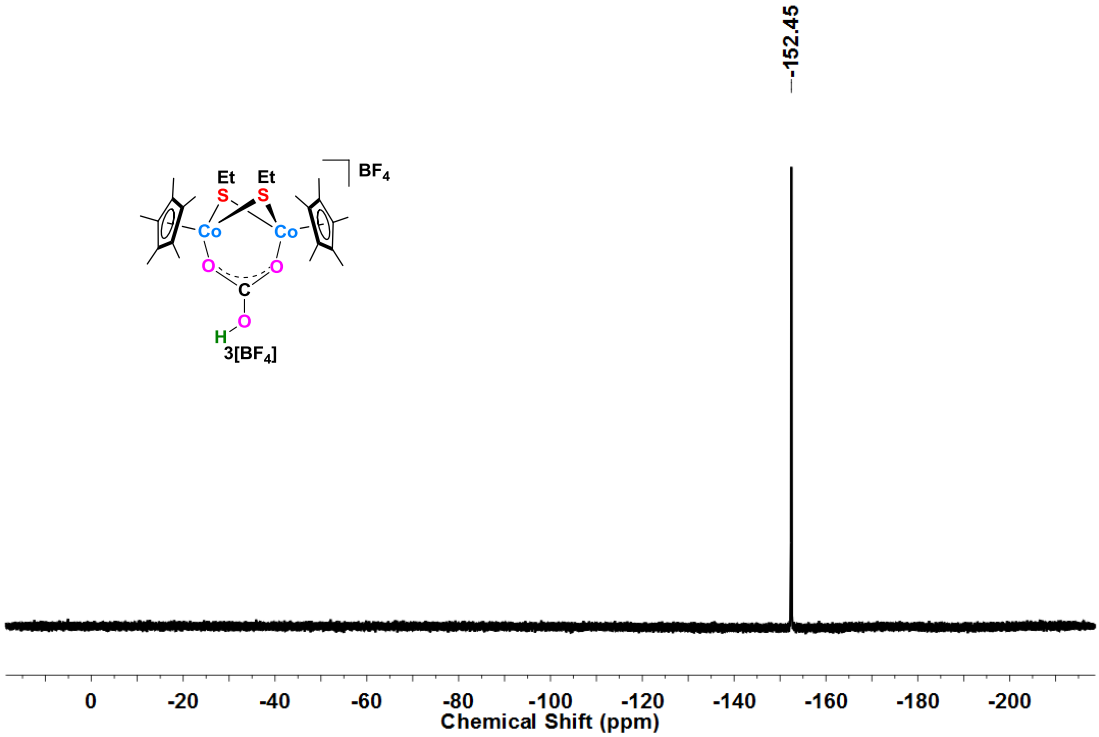

Fig. S17. ^{1}H NMR spectrum of **4[BF$_4$]** in CD_2Cl_2

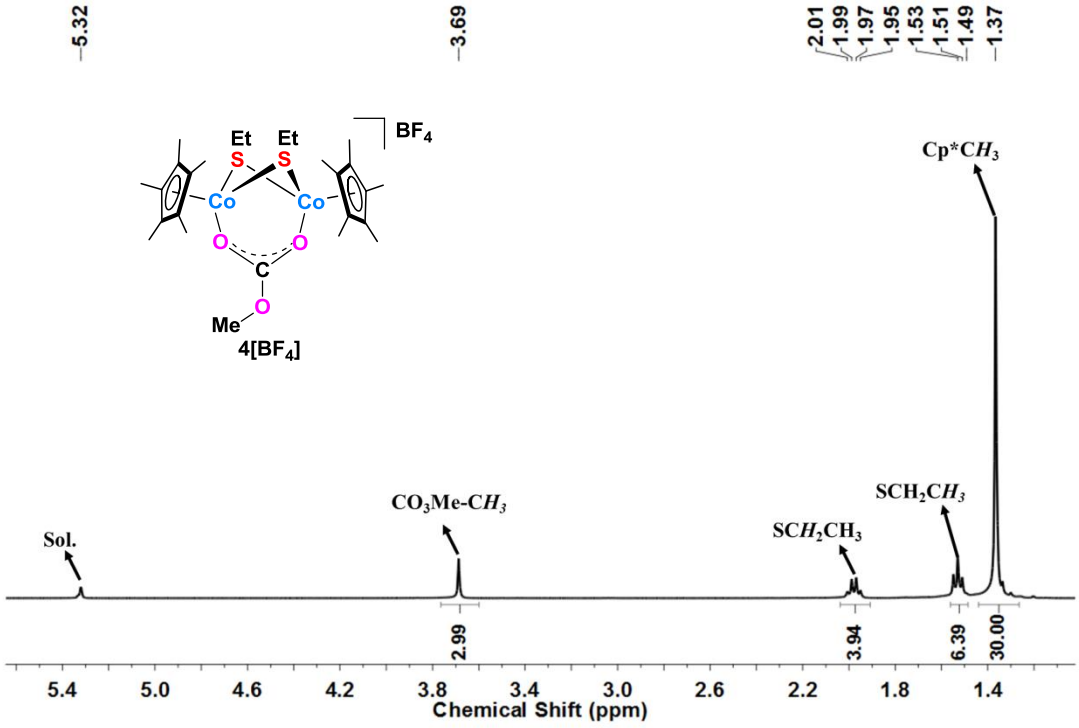

Fig. S18. ^{13}C NMR spectrum of **4[BF$_4$]** in CD_2Cl_2

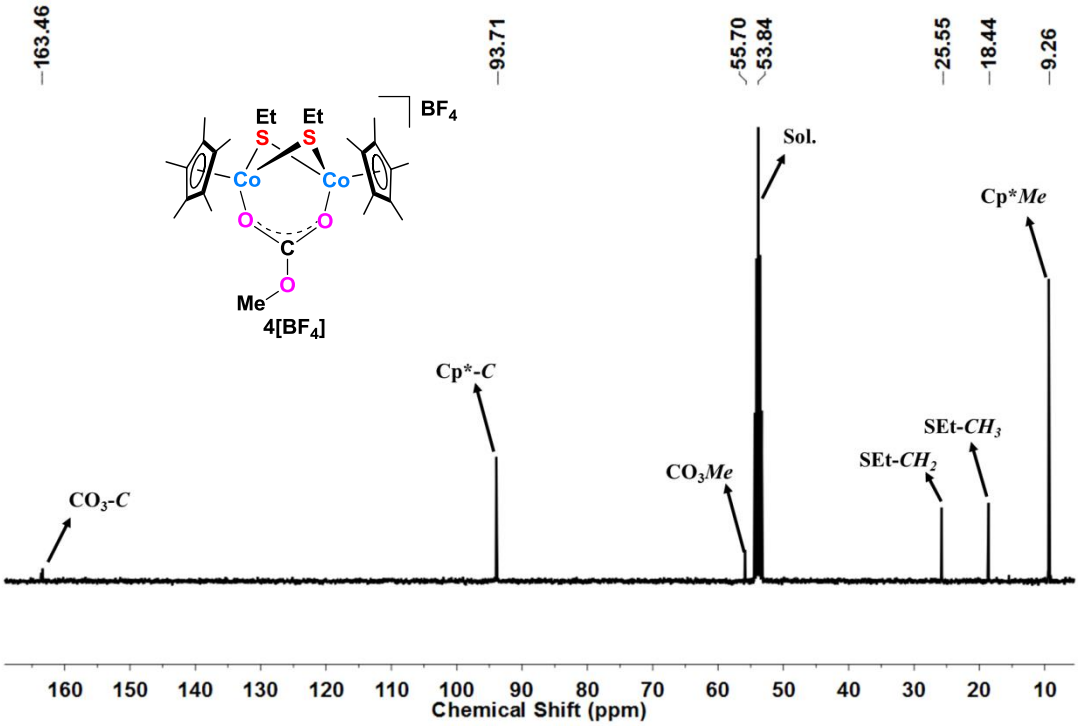

Fig. S19. ^{19}F NMR spectrum of **4[BF$_4$]** in CD_2Cl_2

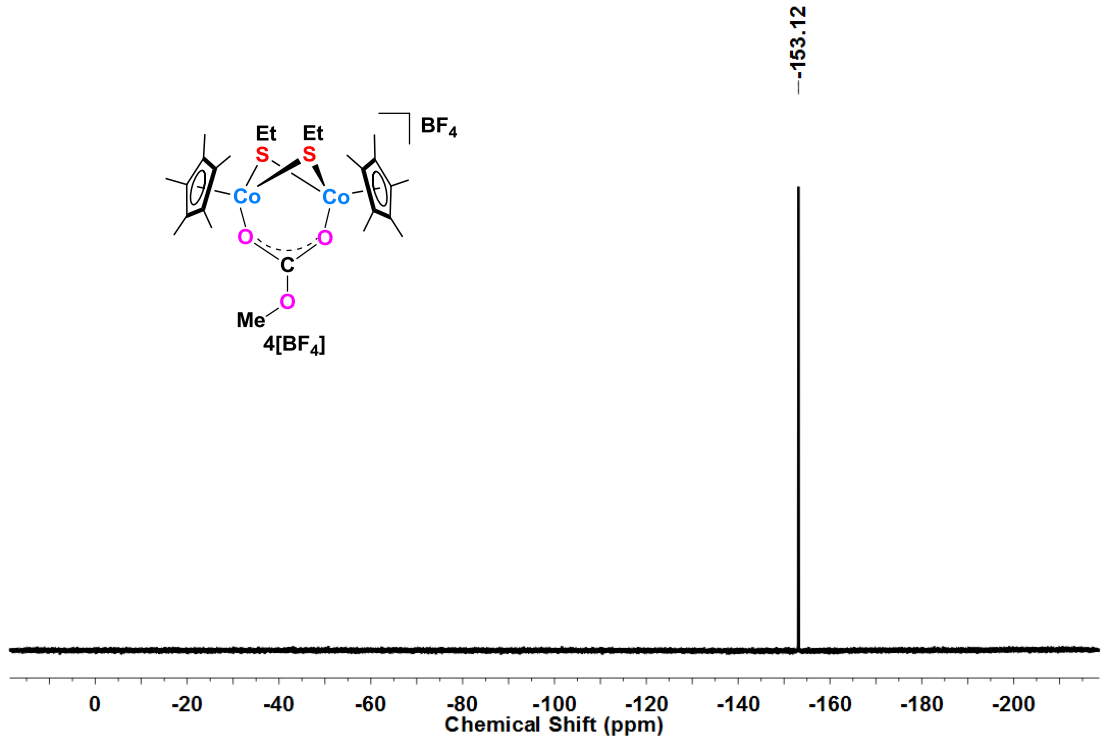

Fig. S20. ^{1}H NMR spectrum of **5a[PF$_6$]** in CD_2Cl_2

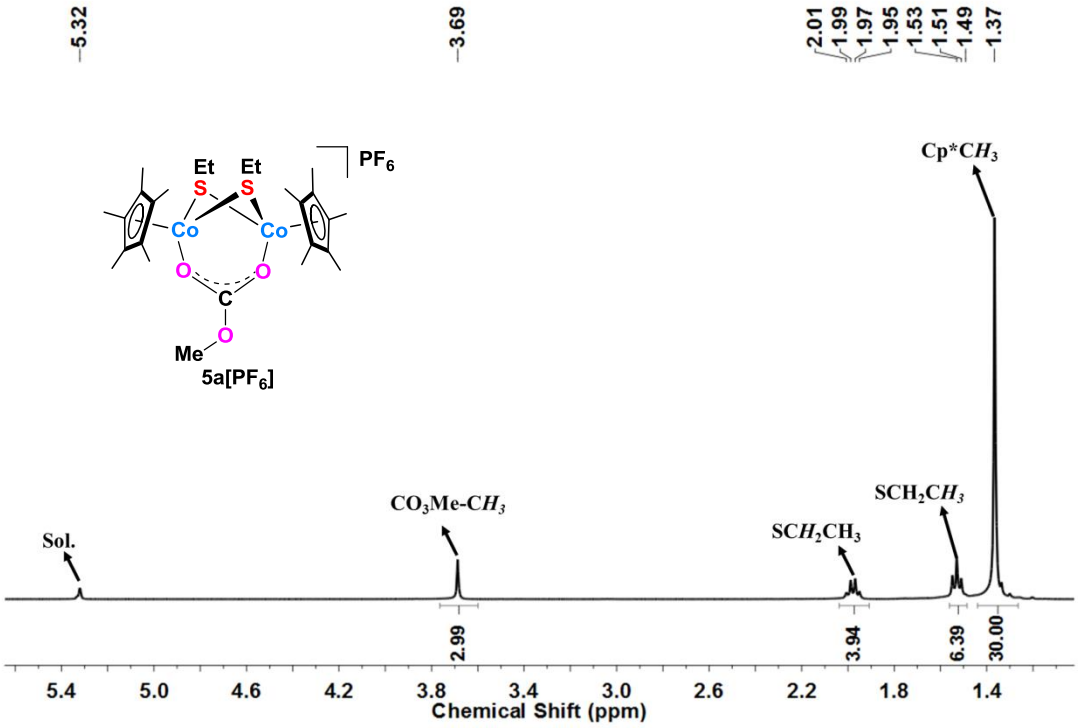

Fig. S21. ^{13}C NMR spectrum of **5a[PF$_6$]** in CD_2Cl_2

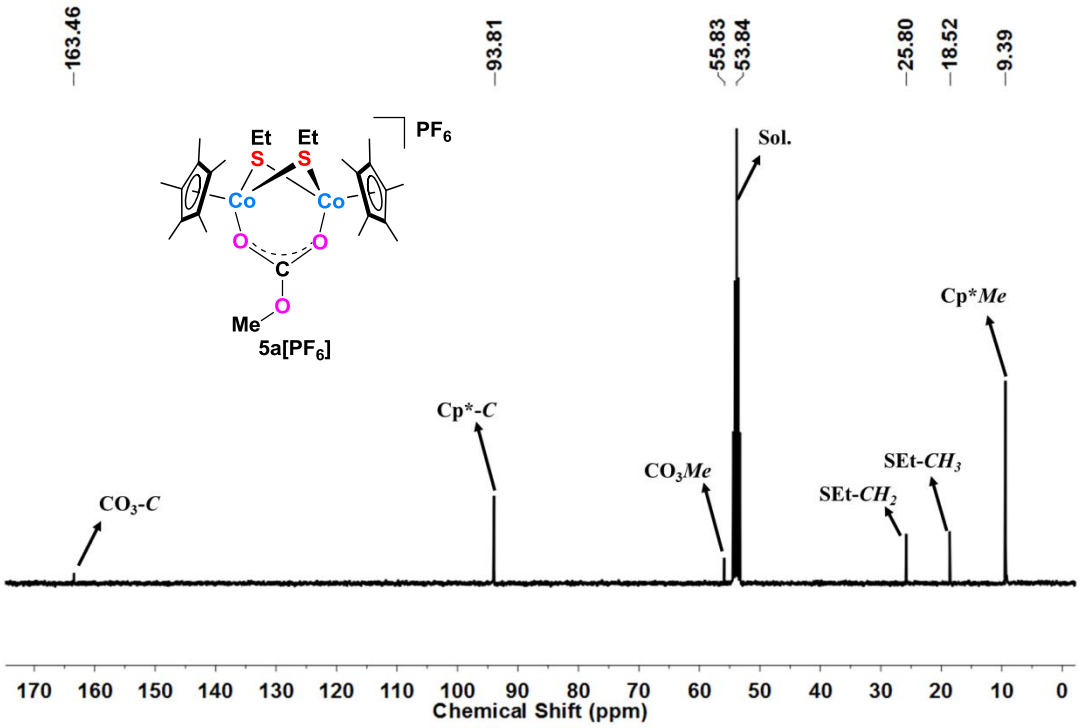

Fig. S22. ^{31}P NMR spectrum of **5a[PF_6]** in CD_2Cl_2

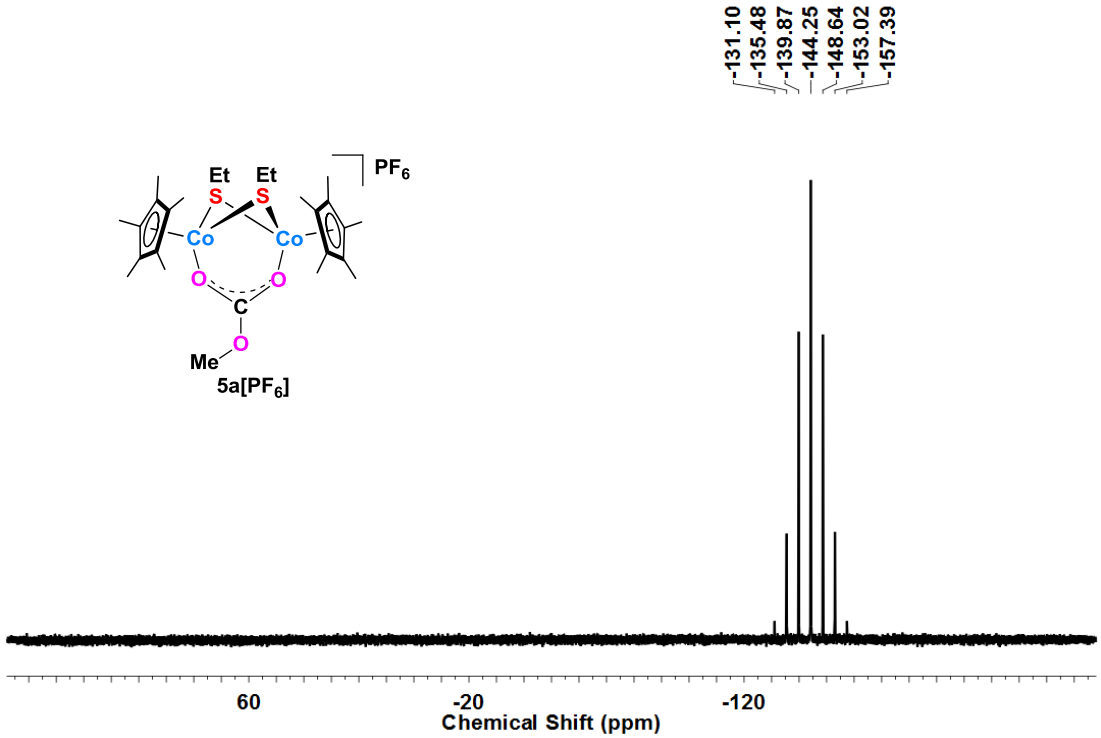

Fig. S23. ^{19}F NMR spectrum of **5a[PF_6]** in CD_2Cl_2

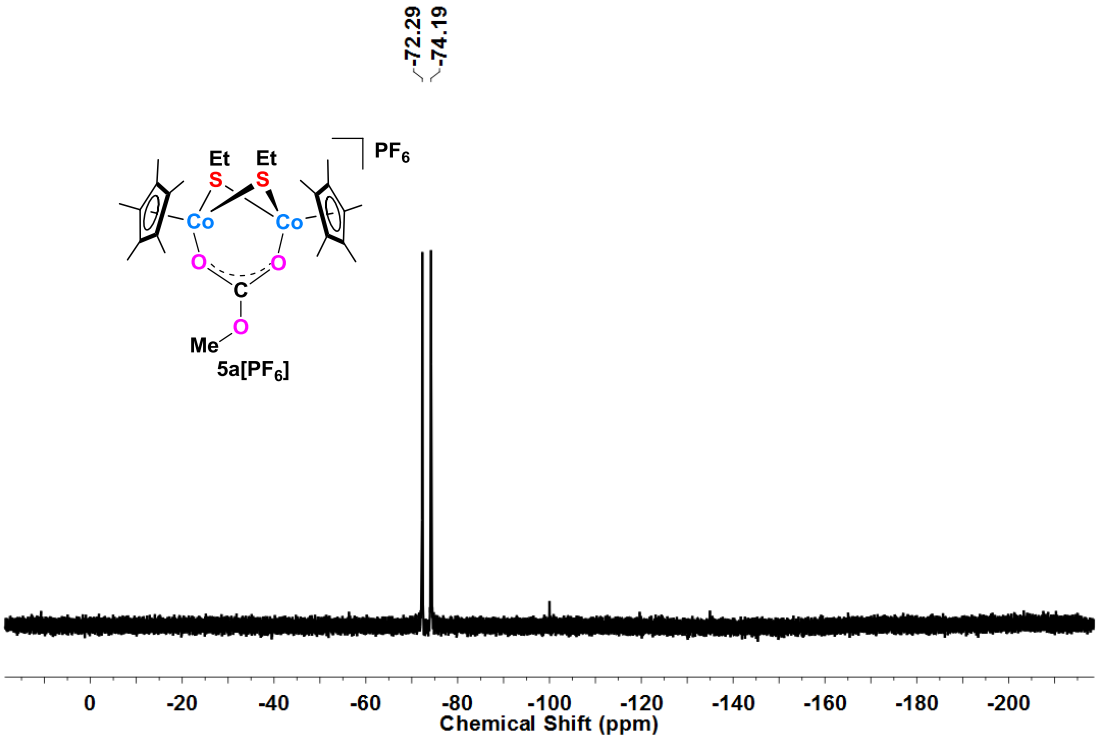

Fig. S24. ^{1}H NMR spectrum of **5b[PF_6]** in CD_2Cl_2

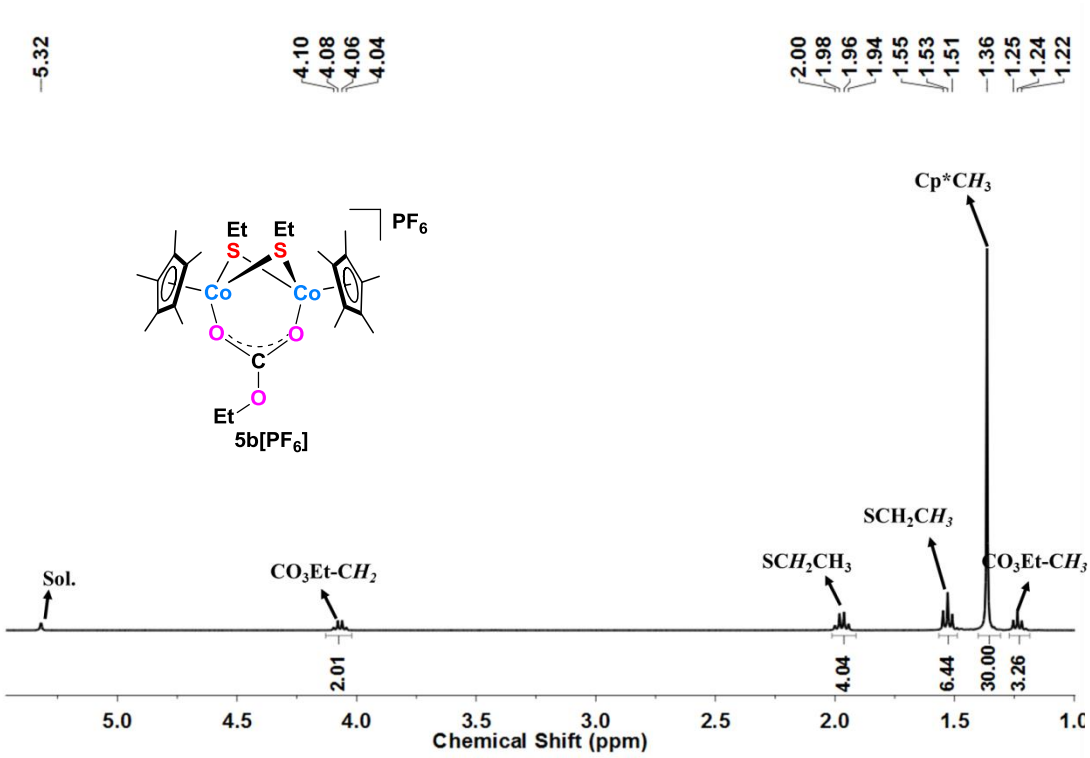

Fig. S25. ^{13}C NMR spectrum of **5b[PF_6]** in CD_2Cl_2

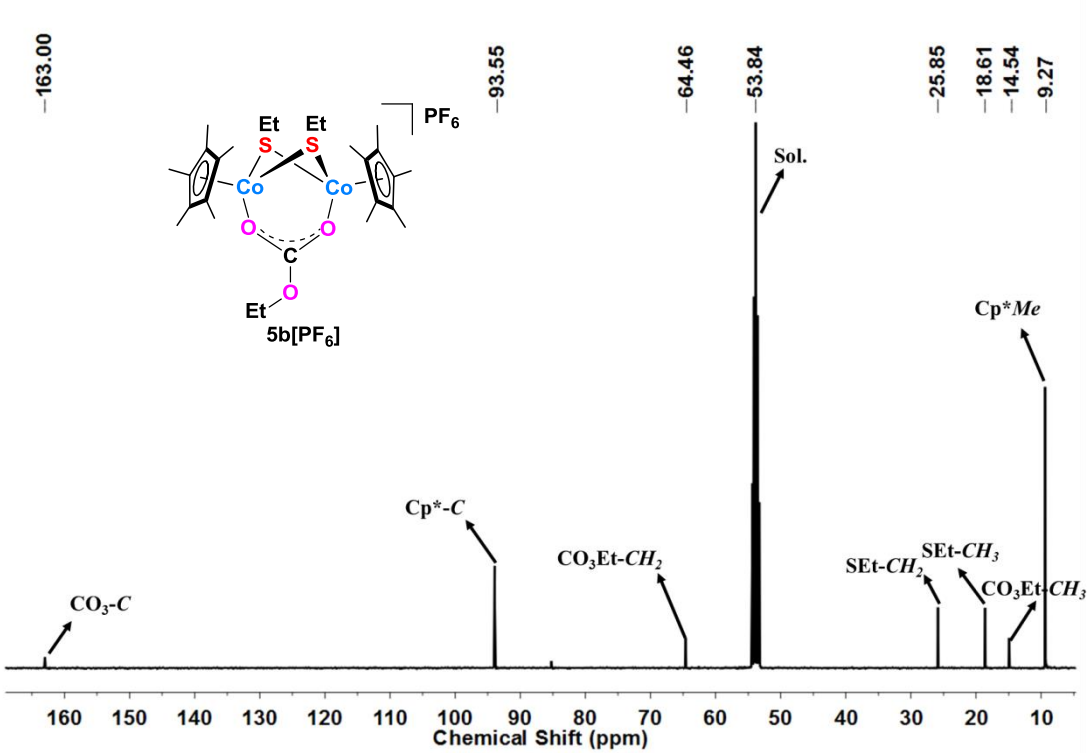

Fig. S26. ^{31}P NMR spectrum of **5b[PF_6]** in CD_2Cl_2

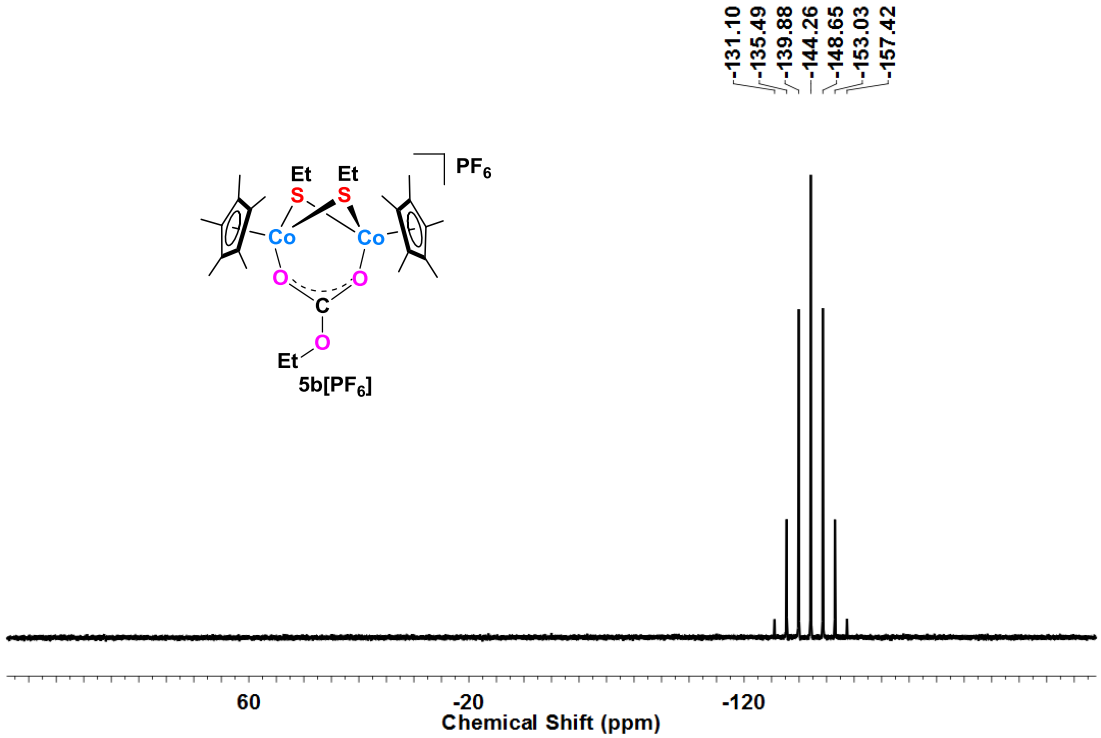

Fig. S27. ^{19}F NMR spectrum of **5b[PF_6]** in CD_2Cl_2

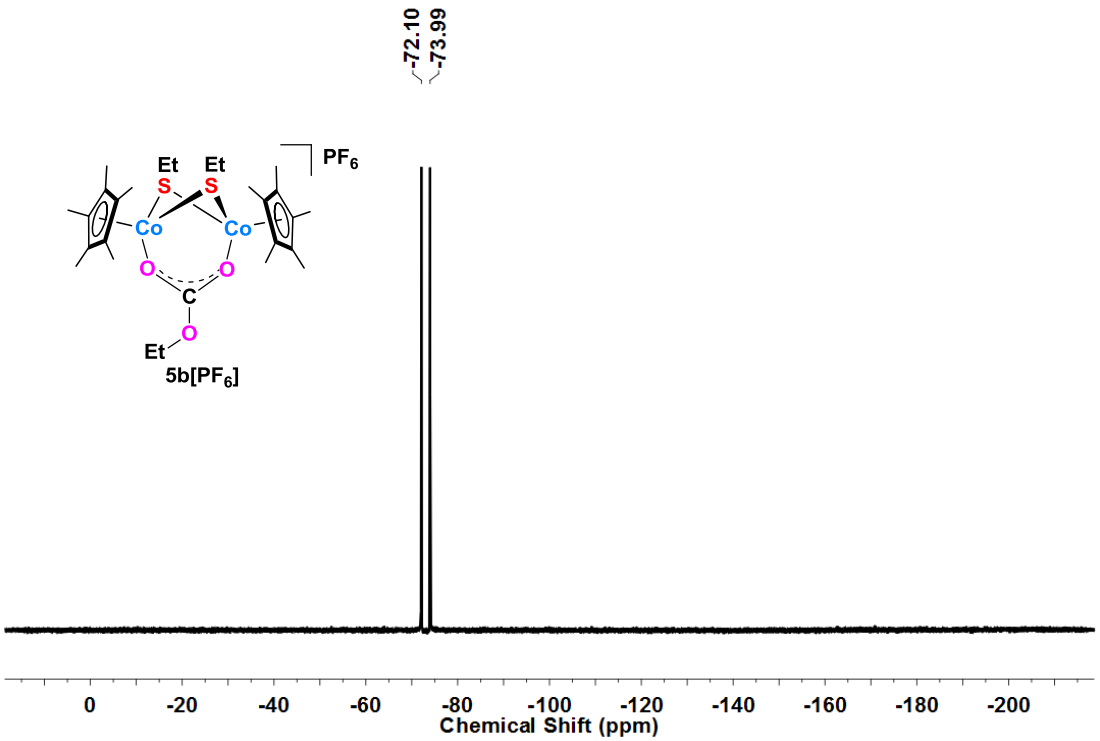

Fig. S28. ^{1}H NMR spectrum of **6a[PF$_6$]** in CD_2Cl_2

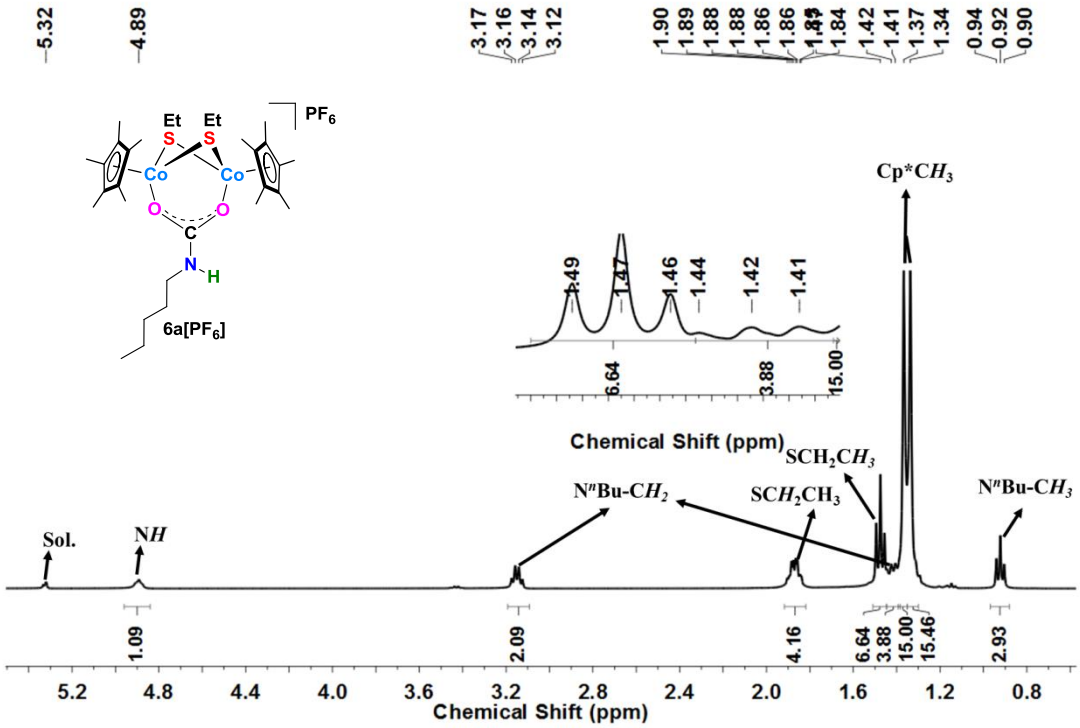

Fig. S29. ^{13}C NMR spectrum of **6a[PF$_6$]** in CD_2Cl_2

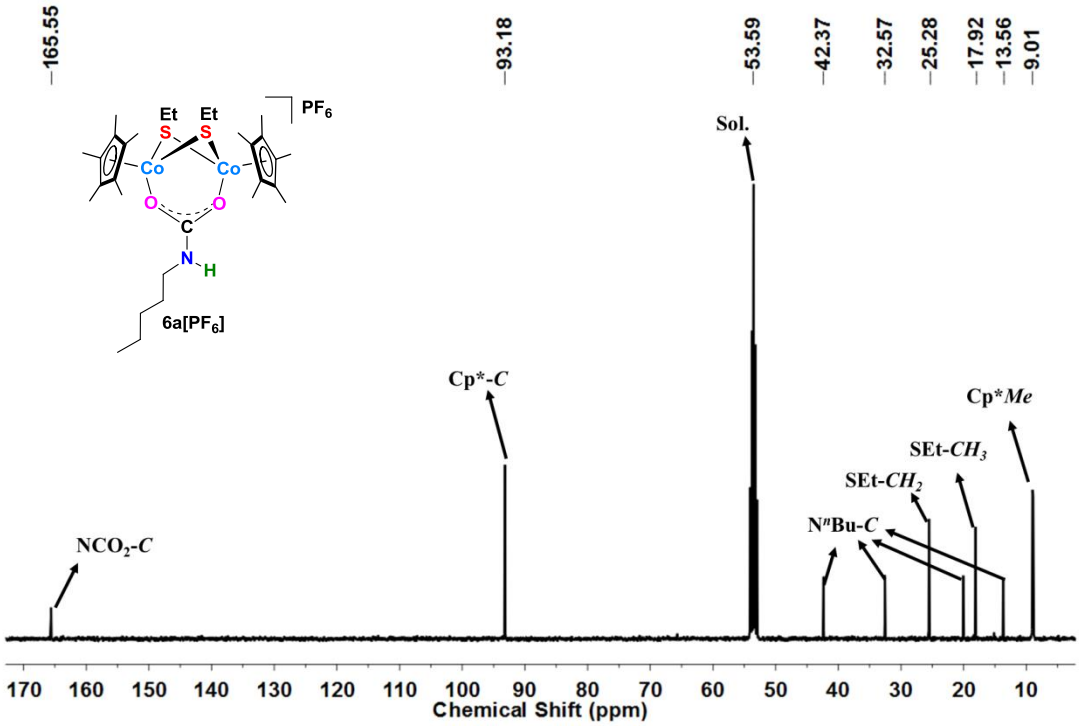

Fig. S30. ^{31}P NMR spectrum of **6a[PF_6]** in CD_2Cl_2

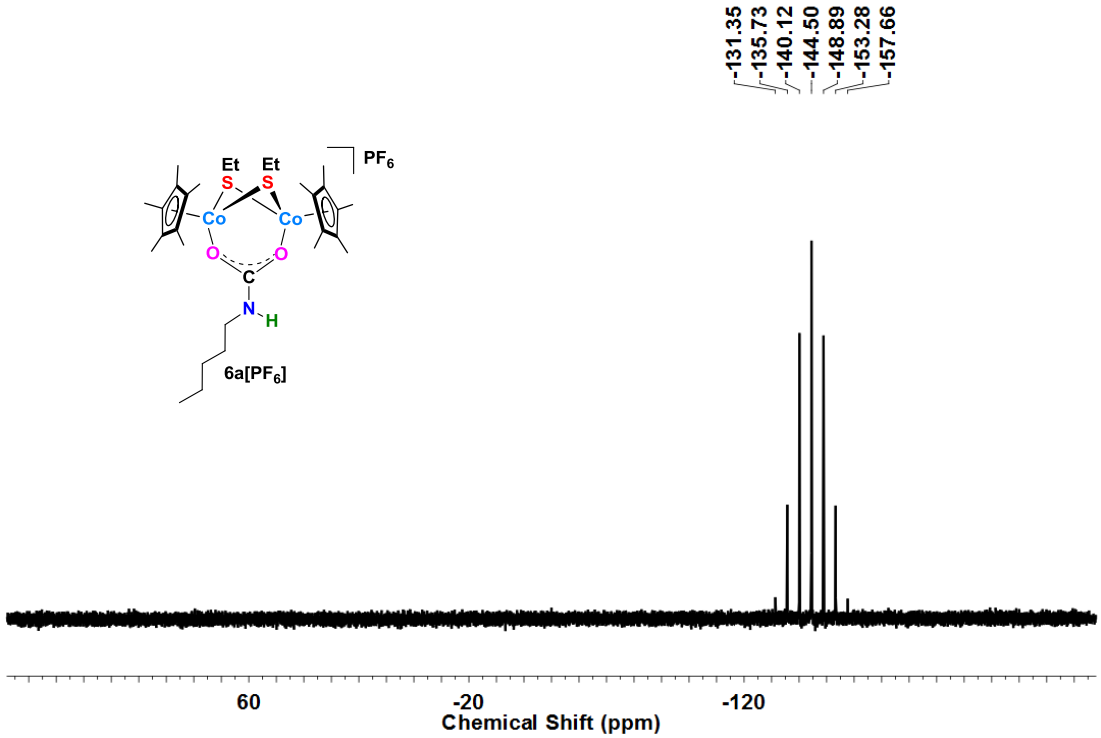

Fig. S31. ^{19}F NMR spectrum of **6a[PF_6]** in CD_2Cl_2

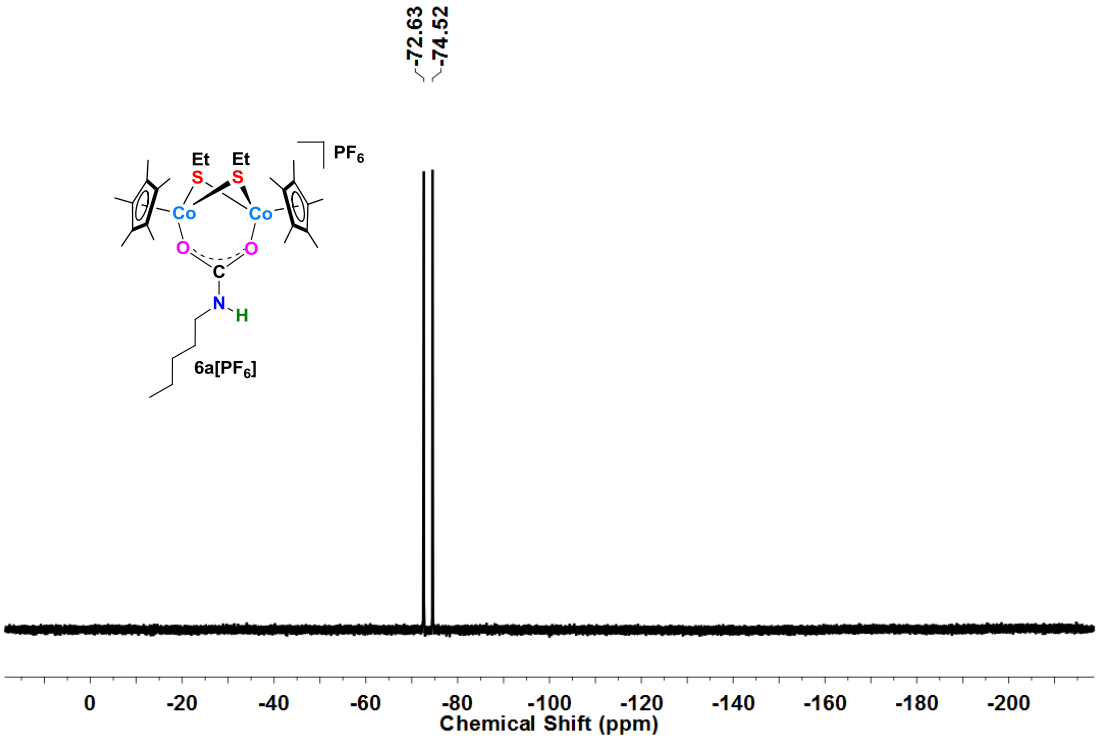

Fig. S32. ^{1}H NMR spectrum of **6b[PF$_6$]** in CD_2Cl_2

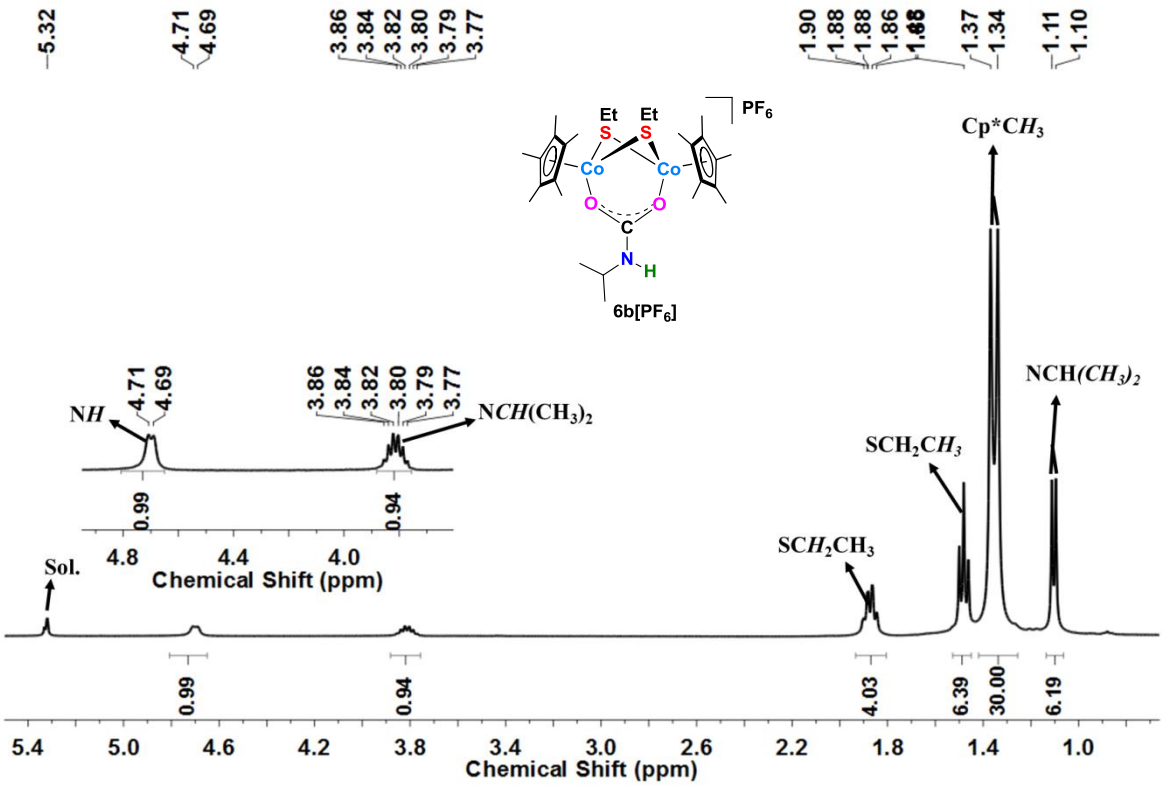

Fig. S33. ^{13}C NMR spectrum of **6b[PF$_6$]** in CD_2Cl_2

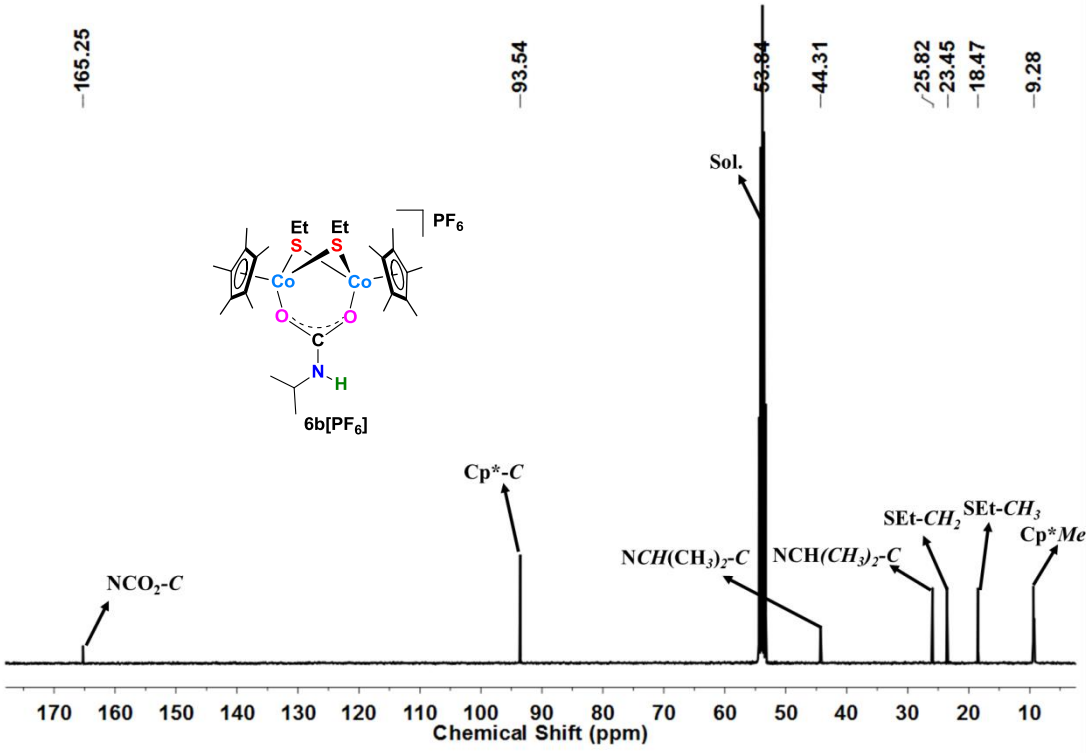

Fig. S34. ^{31}P NMR spectrum of **6b[PF_6]** in CD_2Cl_2

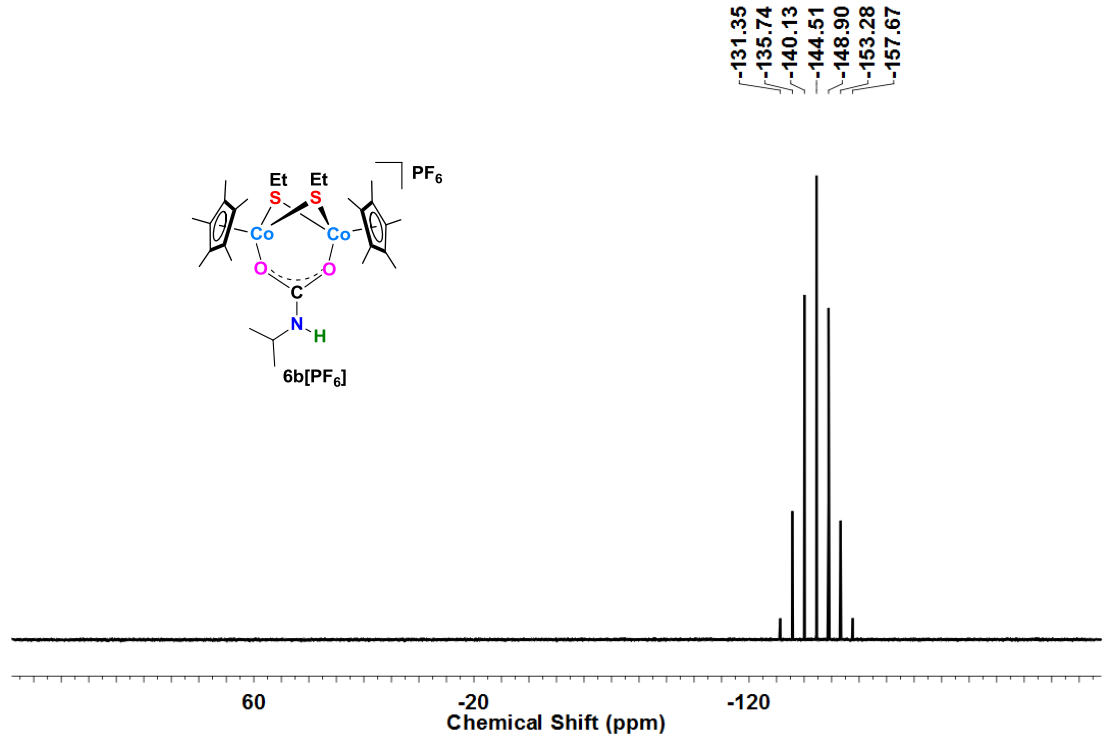

Fig. S35. ^{19}F NMR spectrum of **6b[PF_6]** in CD_2Cl_2

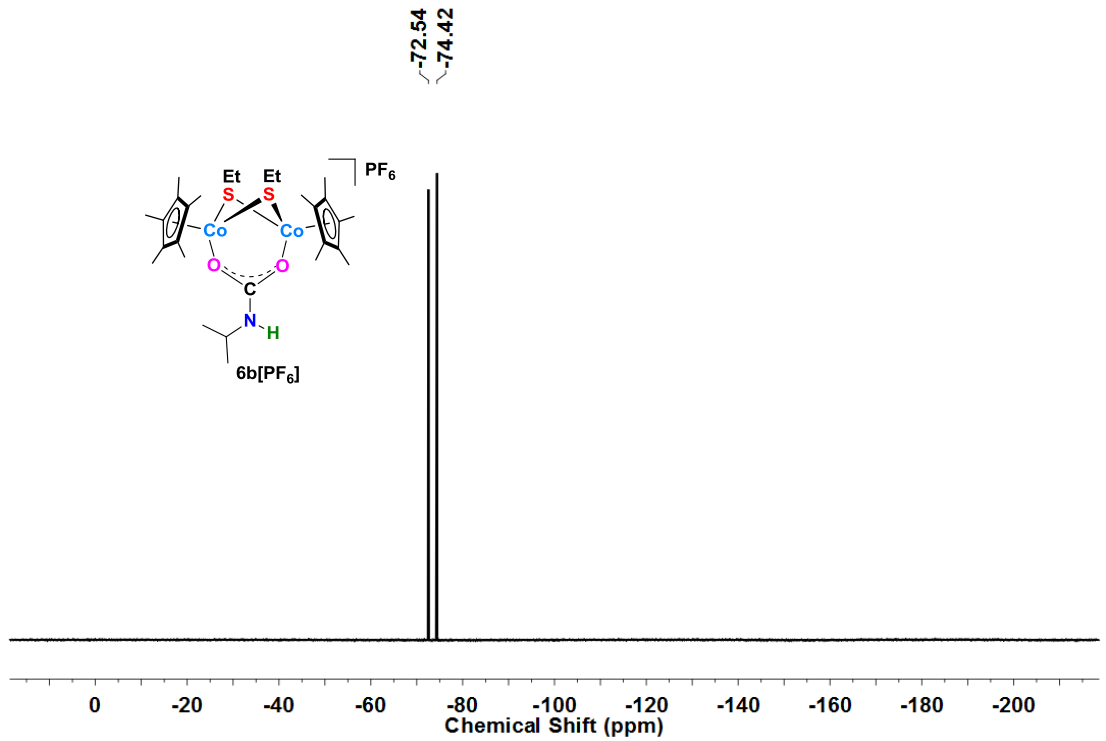

Fig. S36. ^{1}H NMR spectrum of **6c[PF_6]** in CD_2Cl_2

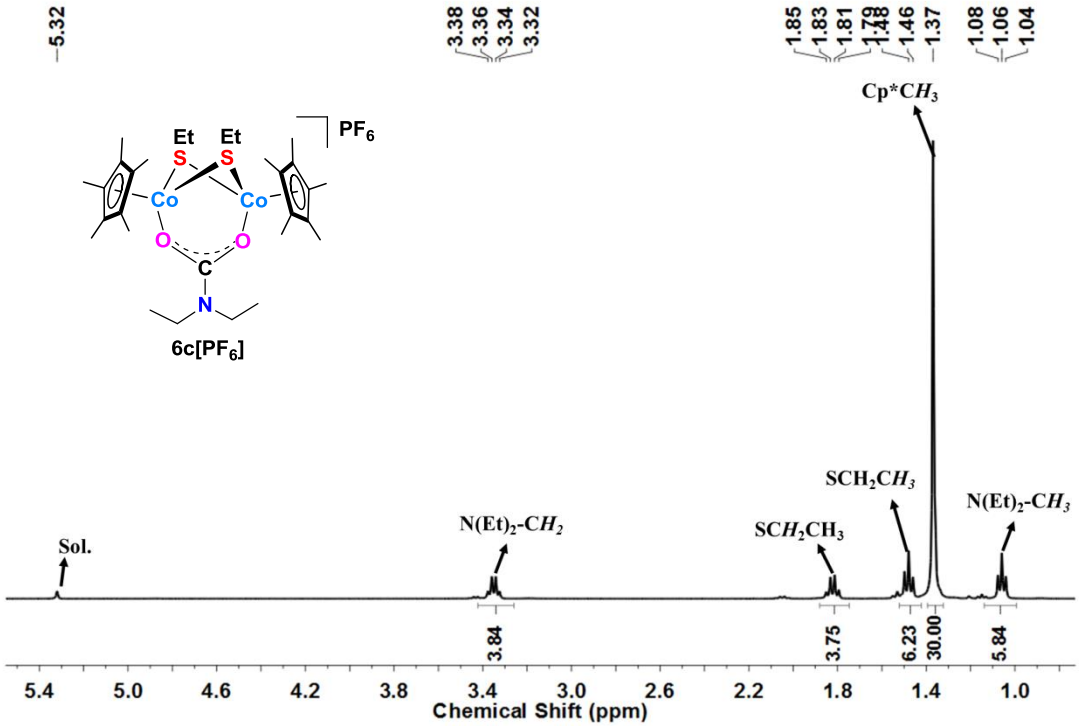

Fig. S37. ^{13}C NMR spectrum of **6c[PF_6]** in CD_2Cl_2

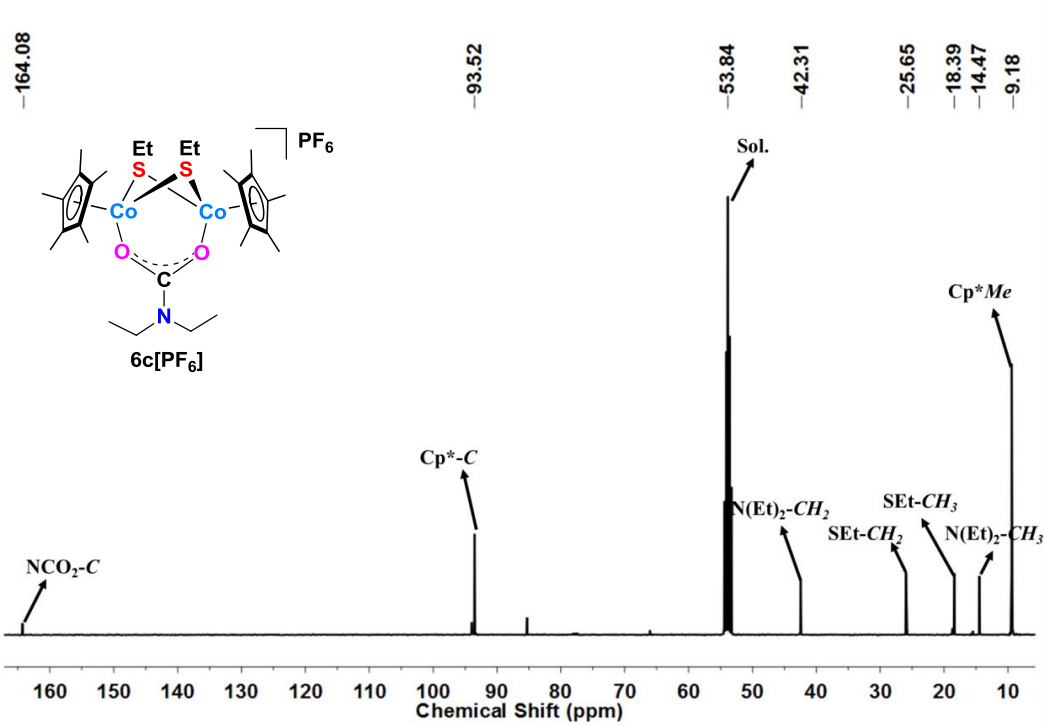

Fig. S38. ^{31}P NMR spectrum of **6c[PF$_6$]** in CD_2Cl_2

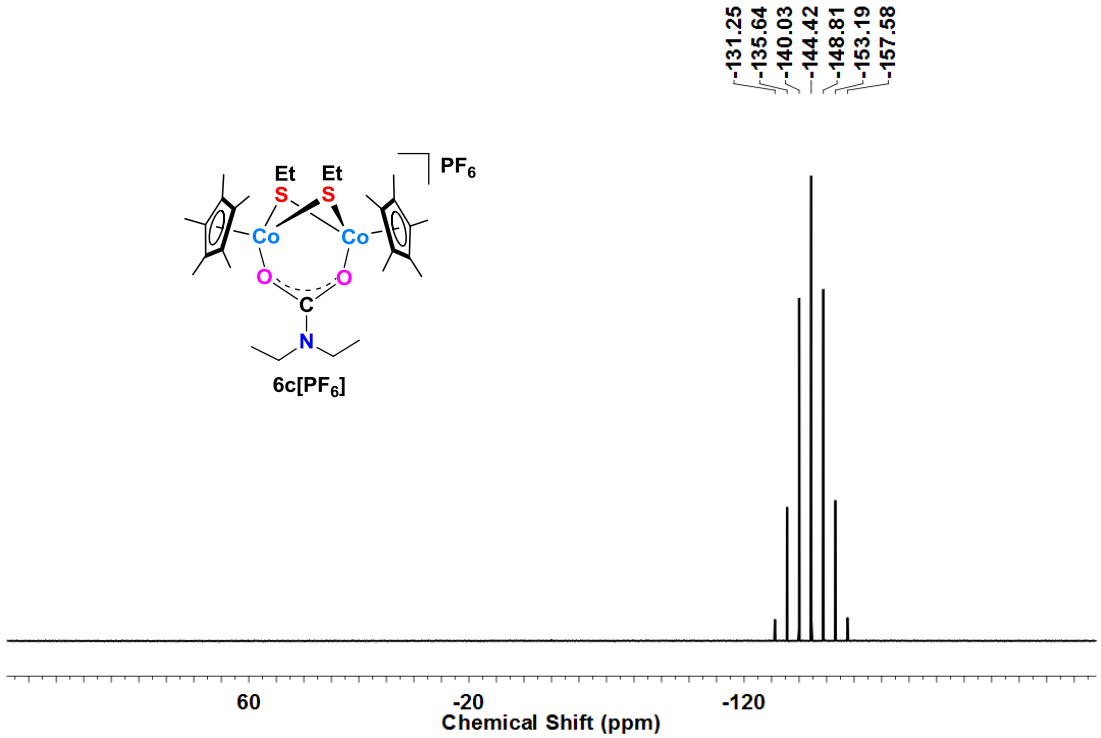

Fig. S39. ^{19}F NMR spectrum of **6c[PF$_6$]** in CD_2Cl_2

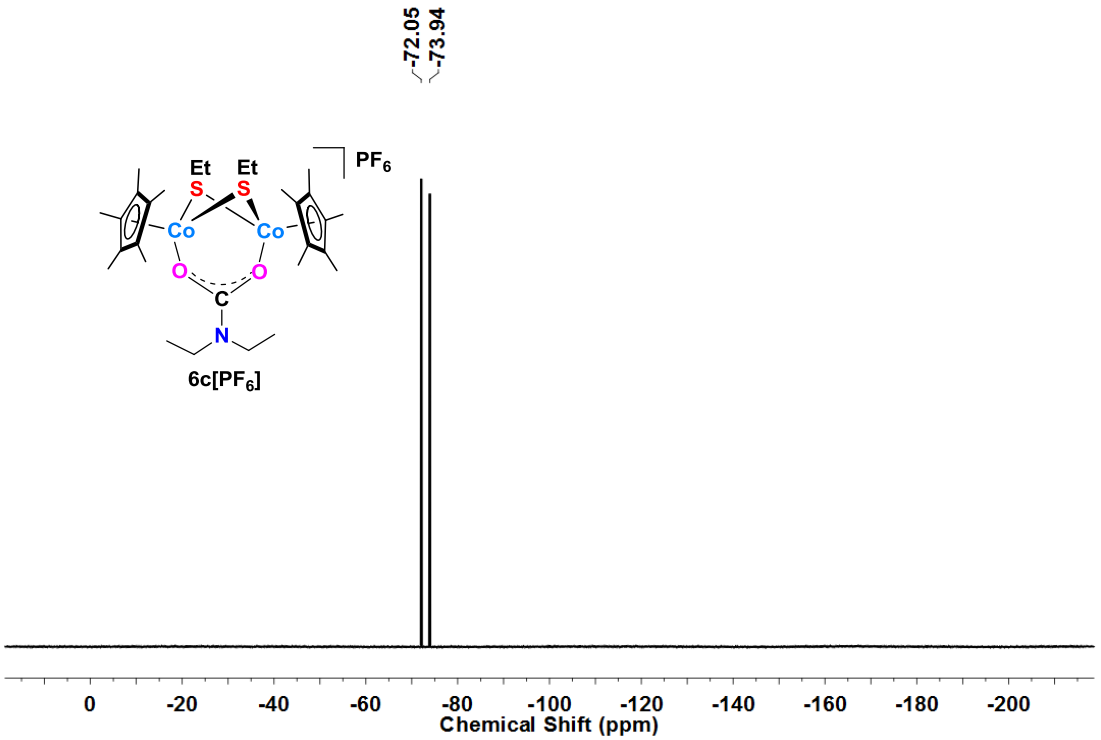

III. ESI-HRMS Spectra

Fig. S40. ESI-HRMS of **3[BF$_4$]** in CH_2Cl_2

(a) The signal at an *m/z* = 571.1169 corresponds to [**3**]$^+$. (b) Calculated isotopic distribution for [**3**]$^+$ (upper) and the amplifying diagram for [**3**]$^+$ (bottom).

(a)

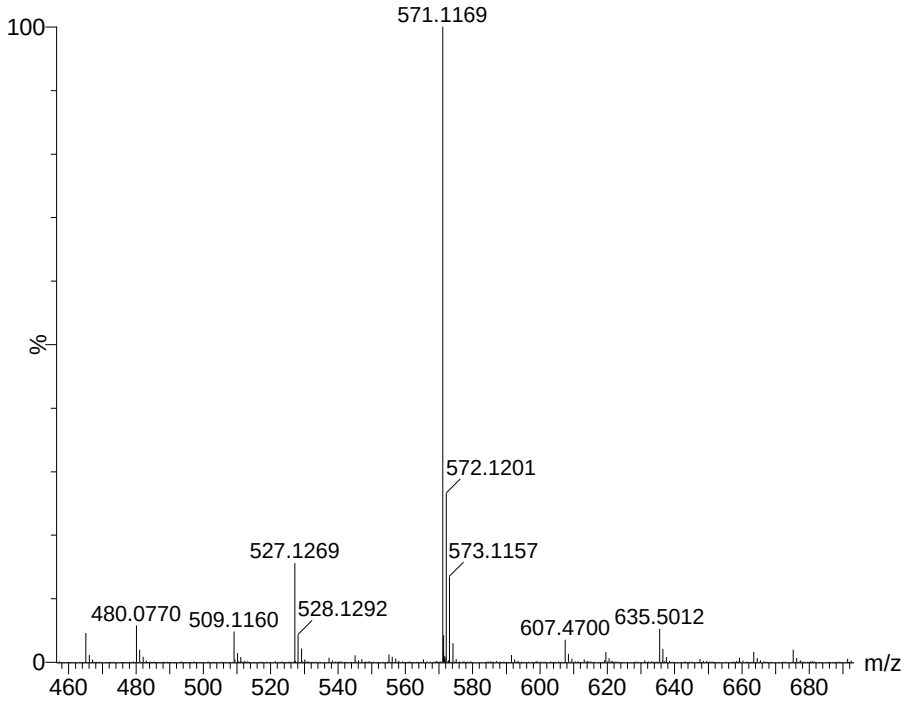

(b)

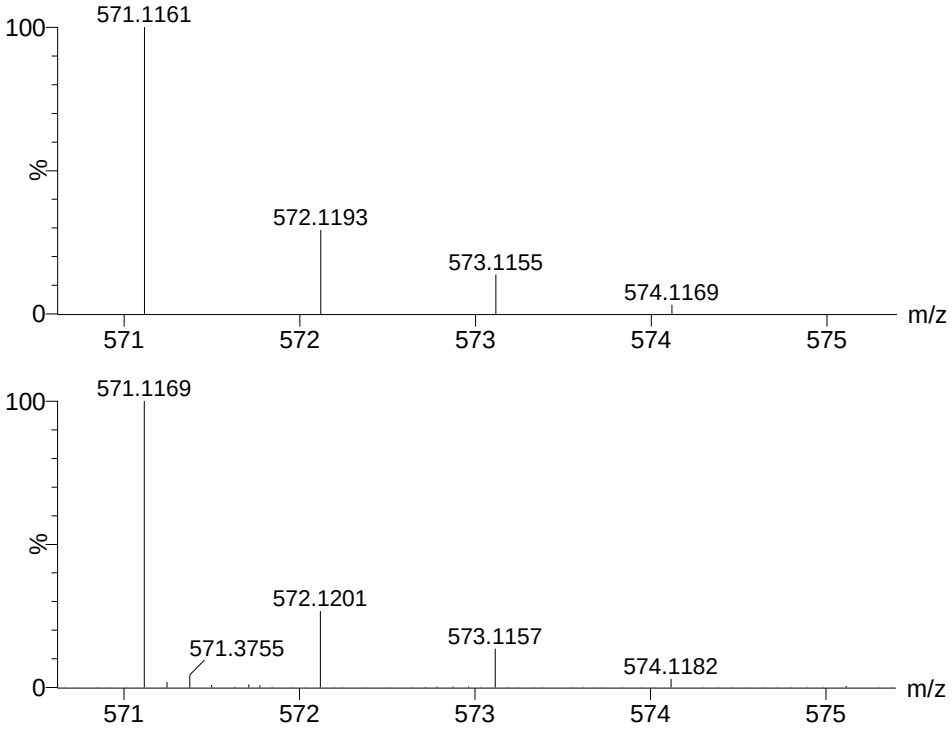

Fig. S41. ESI-HRMS of **^{18}O-3[BF$_4$]** in CH_2Cl_2

(a) The signal at an *m/z* = 573.1201 corresponds to ^{18}O-[**3**]$^+$. (b) Calculated isotopic distribution for ^{18}O-[**3**]$^+$ (upper) and the amplifying diagram for ^{18}O-[**3**]$^+$ (bottom).

(a)

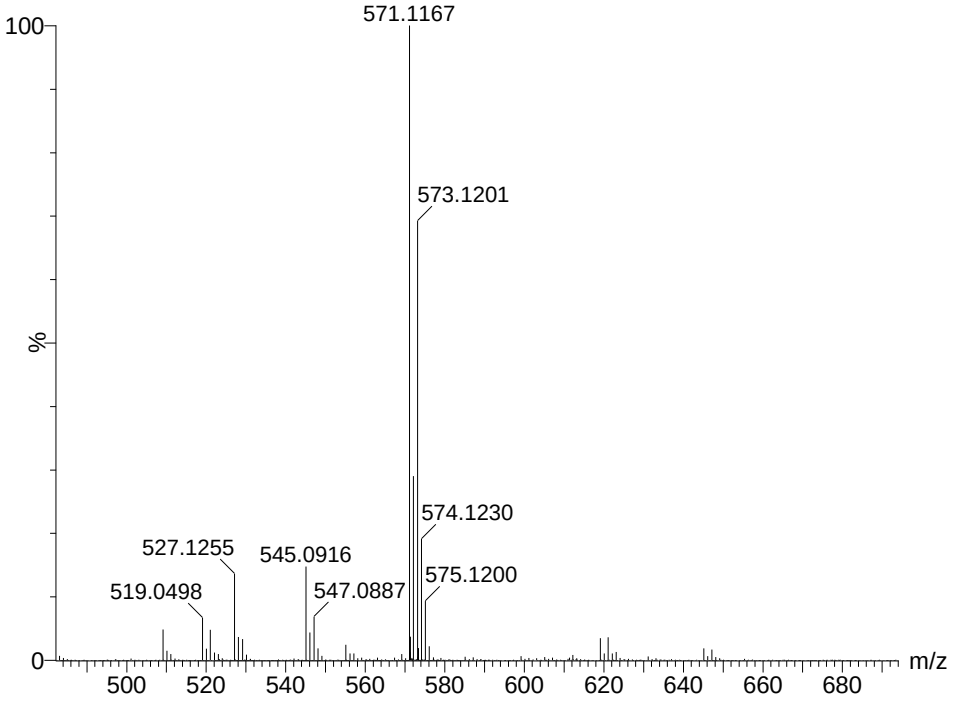

(b)

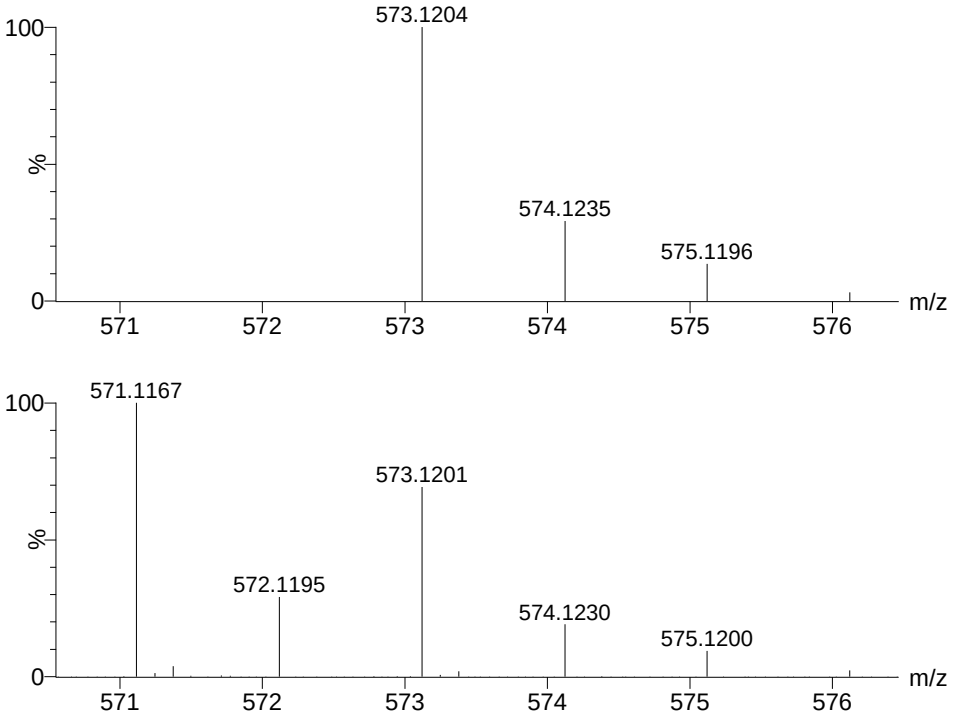

Fig. S42. ESI-HRMS of **4[BF_4]** in CH_2Cl_2

(a) The signal at an *m/z* = 585.1309 corresponds to $[\mathbf{4}]^+$. (b) Calculated isotopic distribution for $[\mathbf{4}]^+$ (upper) and the amplifying diagram for $[\mathbf{4}]^+$ (bottom).

(a)

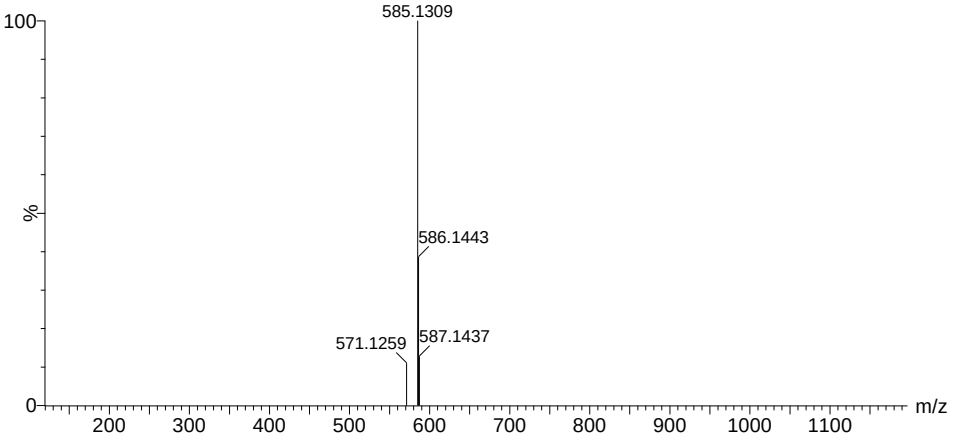

(b)

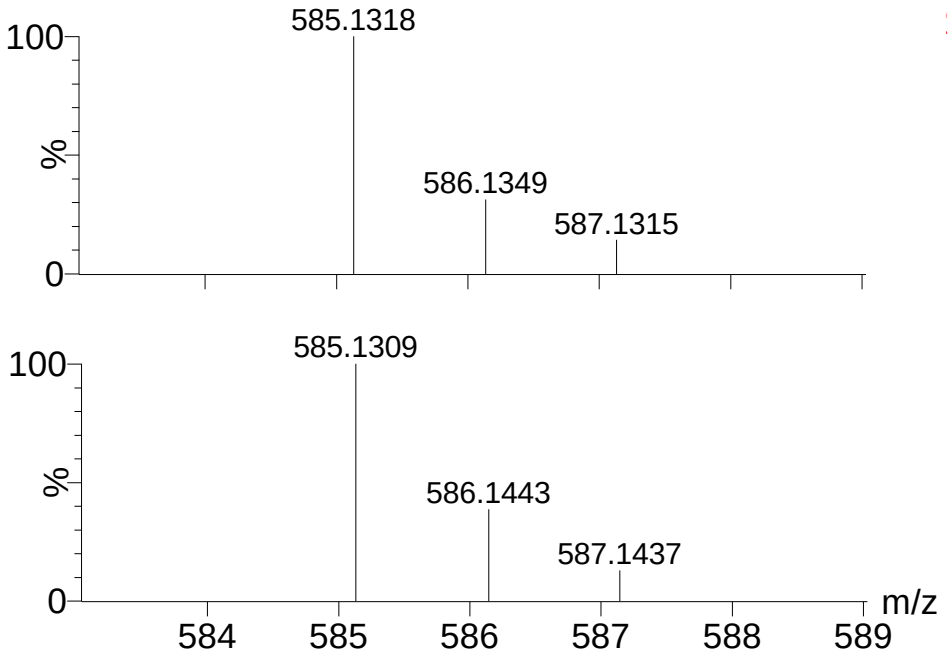

Fig. S43. ESI-HRMS of **^{18}O-4[BF$_4$]** in CH_2Cl_2

(a) The signal at an *m/z* = 587.1346 corresponds to ^{18}O-[**4**]$^+$. (b) Calculated isotopic distribution for ^{18}O-[**4**]$^+$ (upper) and the amplifying diagram for ^{18}O-[**4**]$^+$ (bottom).

(a)

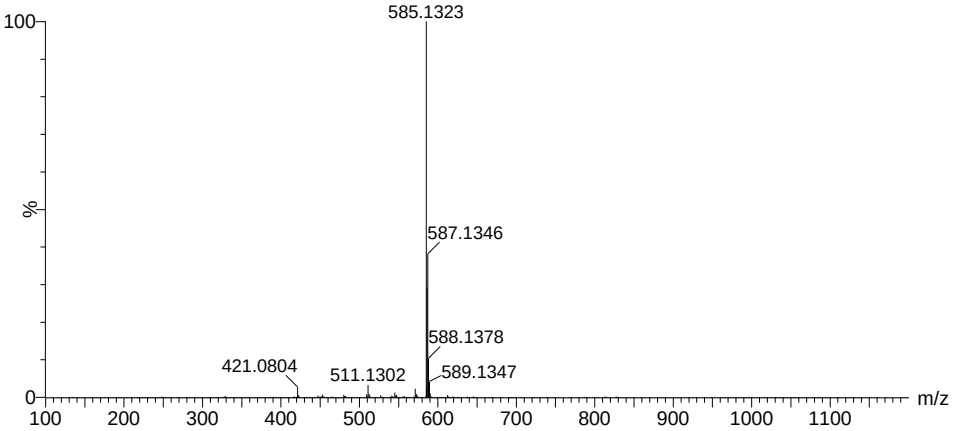

(b)

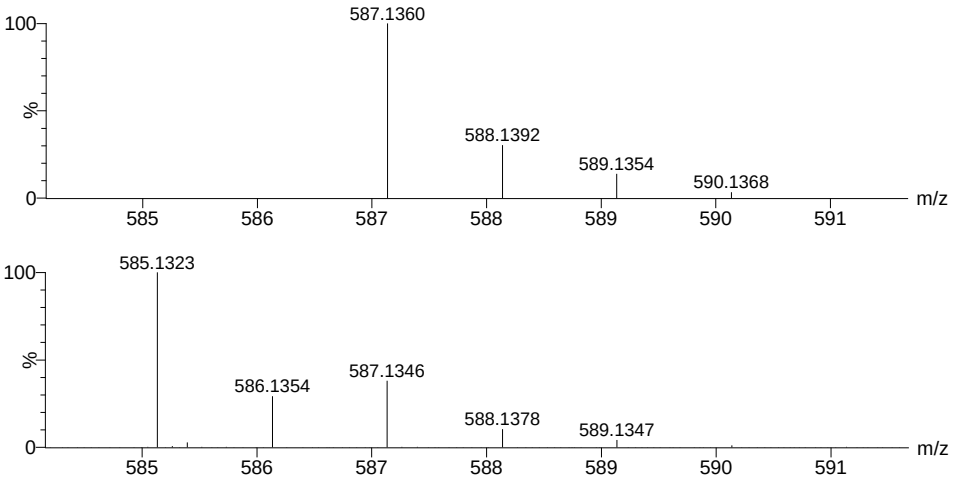

Fig. S44. ESI-HRMS of **5a[PF_6]** in CH_2Cl_2

(a) The signal at an *m/z* = 585.1298 corresponds to [**5a**]$^+$. (b) Calculated isotopic distribution for [**5a**]$^+$ (upper) and the amplifying diagram for [**5a**]$^+$ (bottom).

(a)

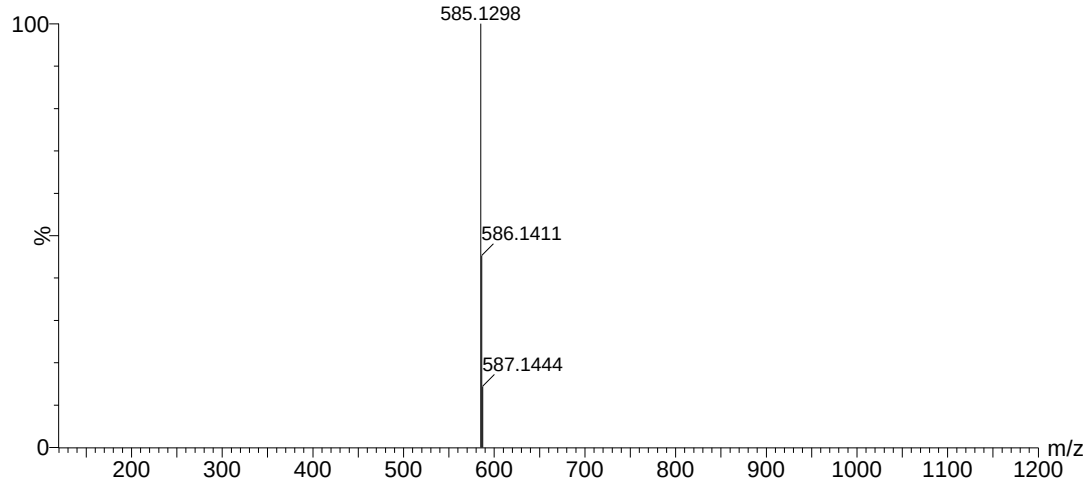

(b)

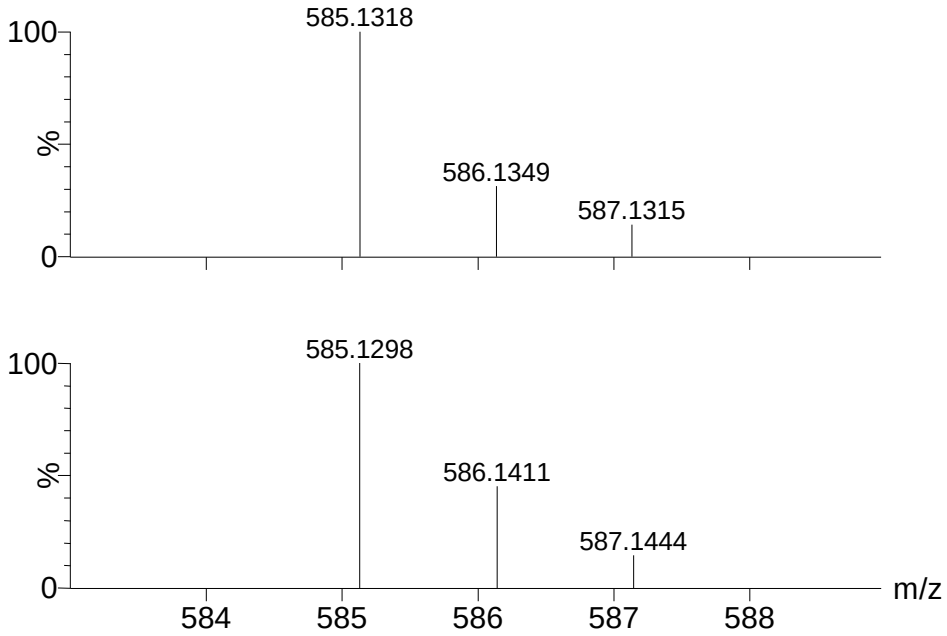

Fig. S45. ESI-HRMS of **5b[PF_6]** in CH_2Cl_2

(a) The signal at an *m/z* = 599.1478 corresponds to [**5b**]$^+$. (b) Calculated isotopic distribution for [**5b**]$^+$ (upper) and the amplifying diagram for [**5b**]$^+$ (bottom).

(a)

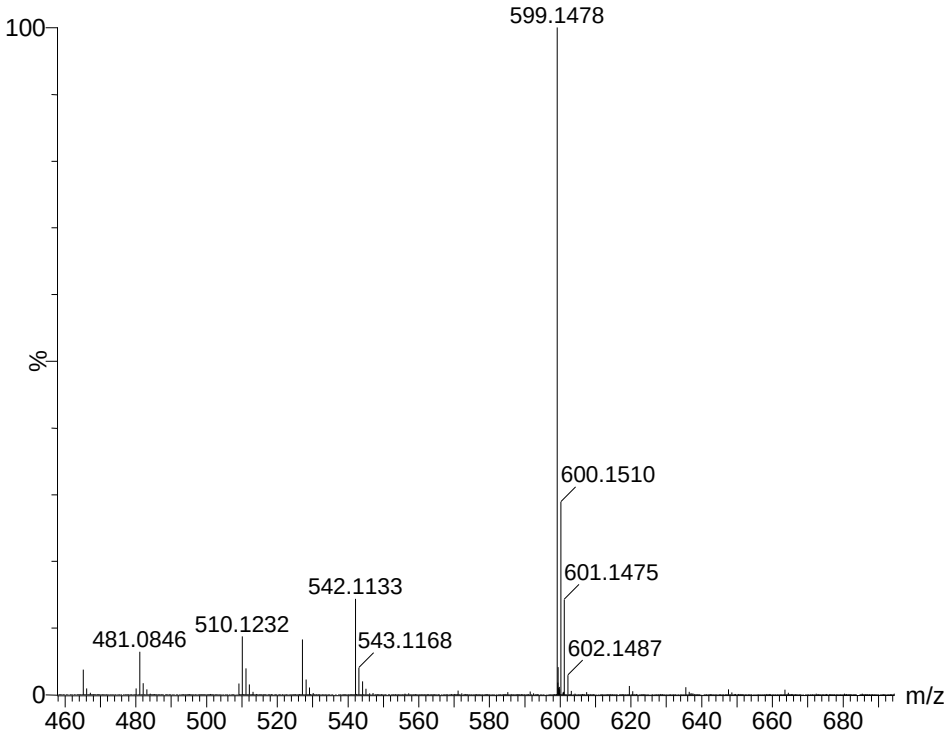

(b)

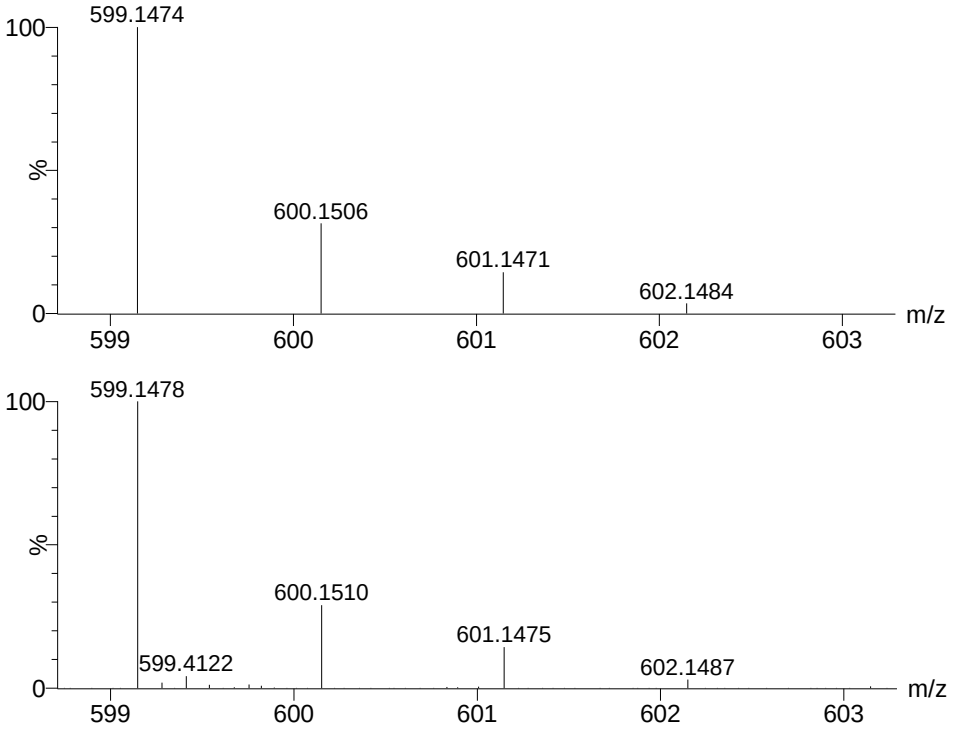

Fig. S46. ESI-HRMS of **6a[PF_6]** in CH_2Cl_2

(a) The signal at an *m/z* = 626.1956 corresponds to [**6a**]$^+$. (b) Calculated isotopic distribution for [**6a**]$^+$ (upper) and the amplifying diagram for [**6a**]$^+$ (bottom).

(a)

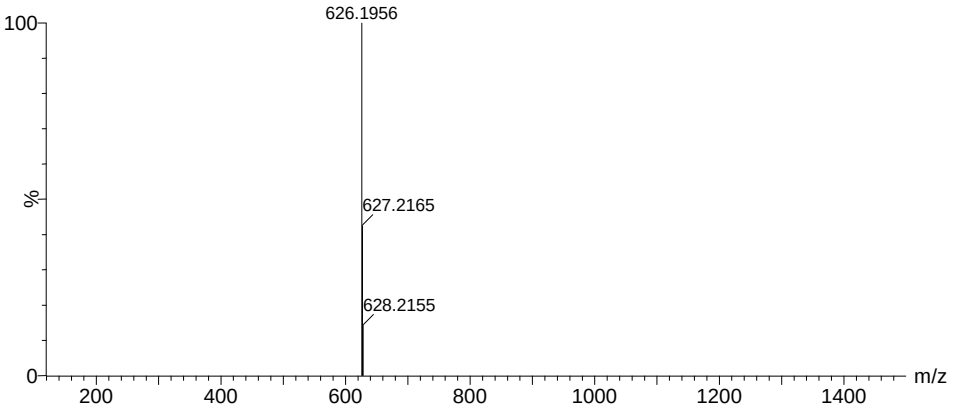

(b)

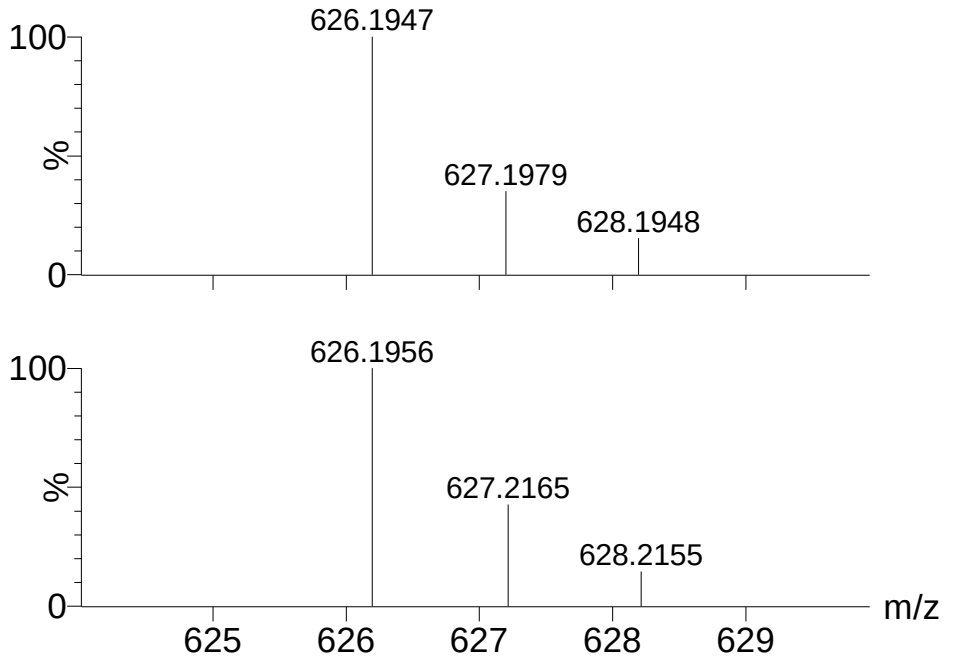

Fig. S47. ESI-HRMS of **6b[PF_6]** in CH_2Cl_2

(a) The signal at an *m/z* = 612.1782 corresponds to [**6b**]$^+$. (b) Calculated isotopic distribution for [**6b**]$^+$ (upper) and the amplifying diagram for [**6b**]$^+$ (bottom).

(a)

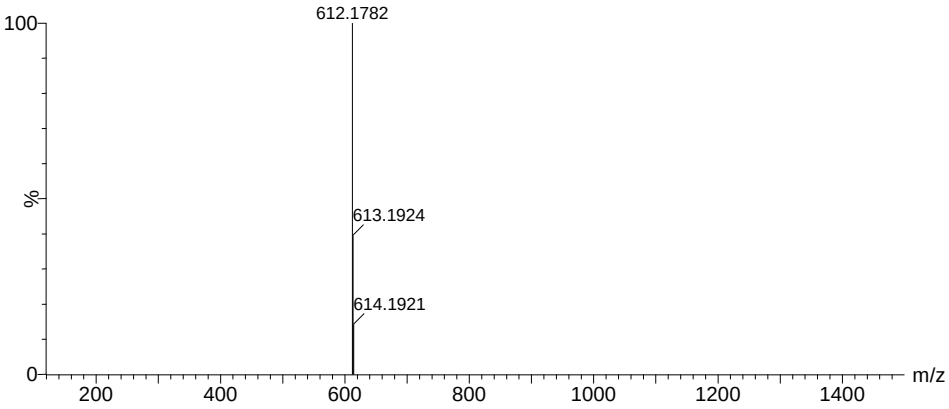

(b)

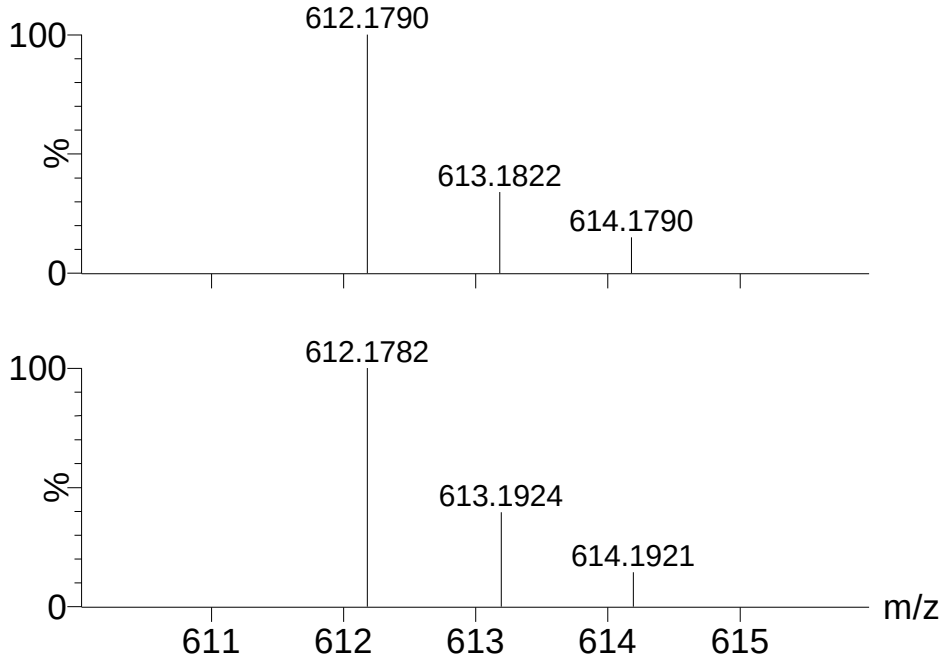

Fig. S48. ESI-HRMS of **6c[PF_6]** in CH_2Cl_2

(a) The signal at an *m/z* = 612.1952 corresponds to [**6c**]$^+$. (b) Calculated isotopic distribution for [**6c**]$^+$ (upper) and the amplifying diagram for [**6c**]$^+$ (bottom).

(a)

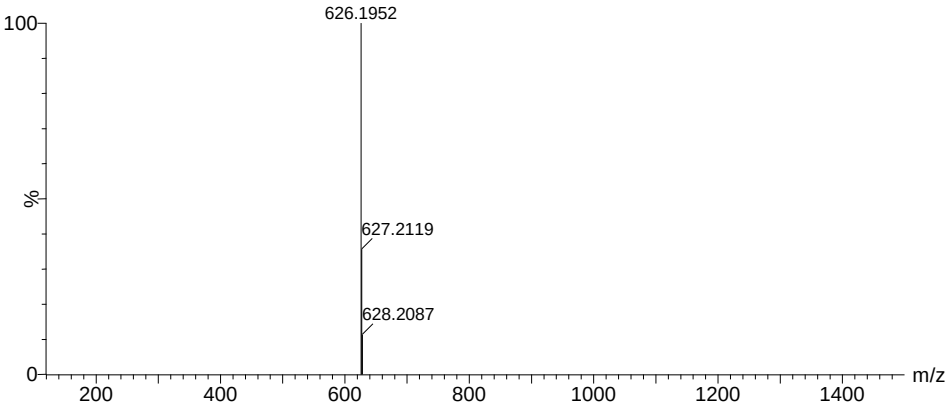

(b)

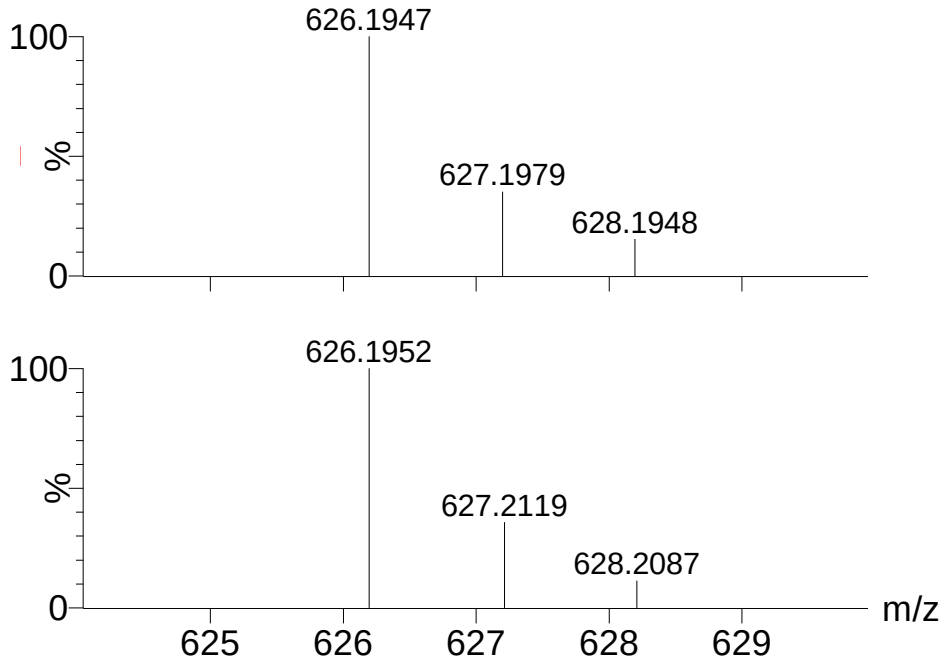

IV. IR(film) Spectra

Fig. S49. IR (film) spectrum of **1**

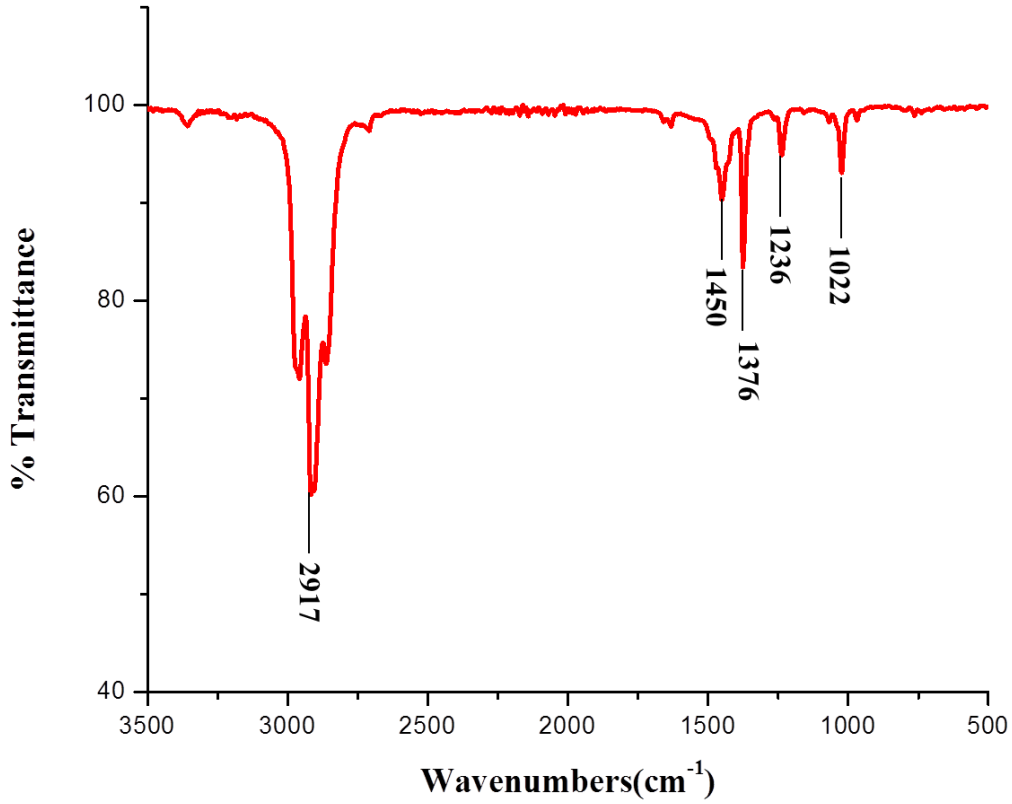

Fig. S50. IR (film) spectrum of **2**

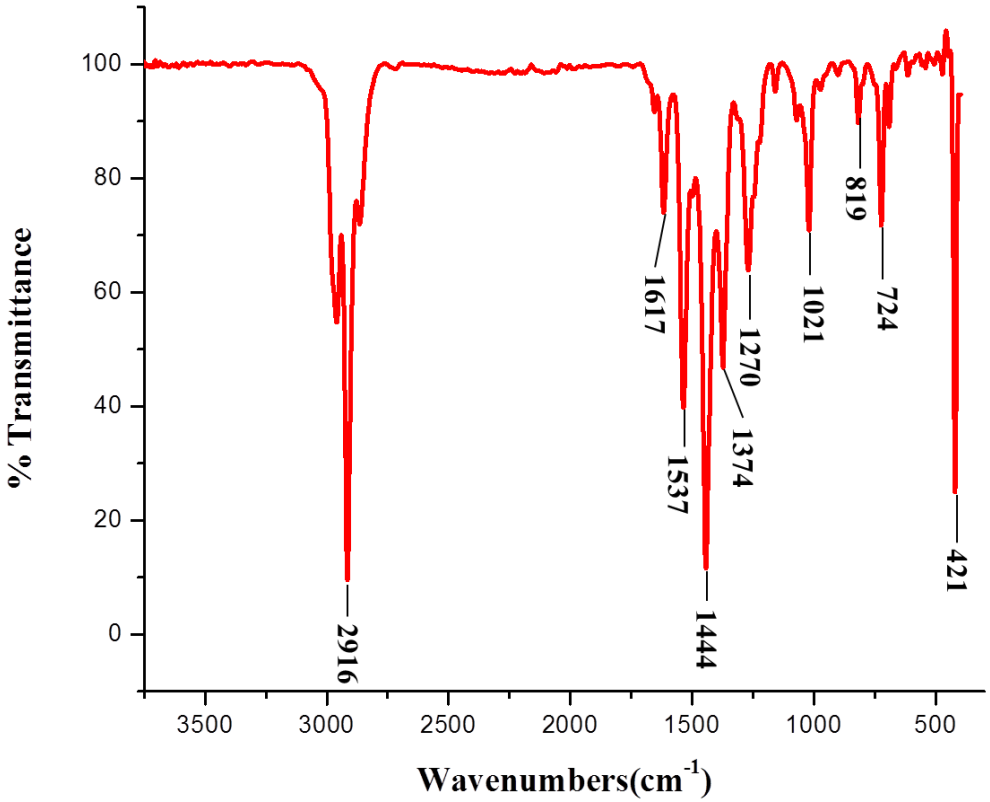

Fig. S51. IR (film) spectrum of ^{18}O-**2**

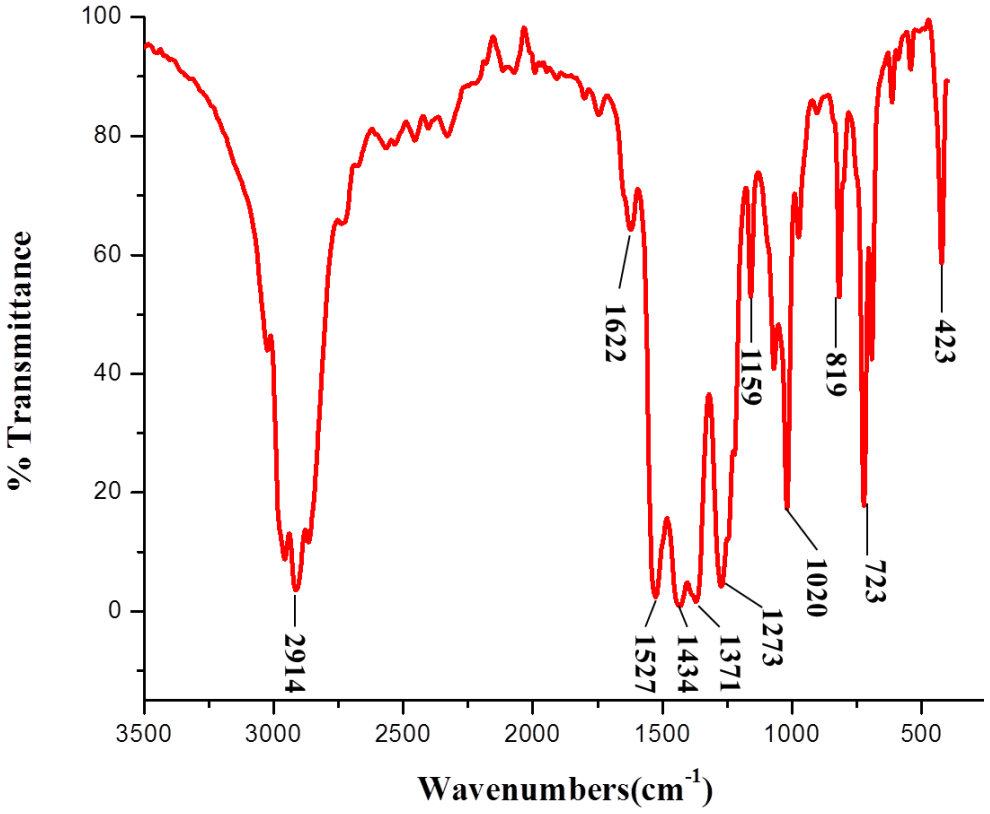

Fig. S52. IR (film) spectrum of **3[BF_4]**

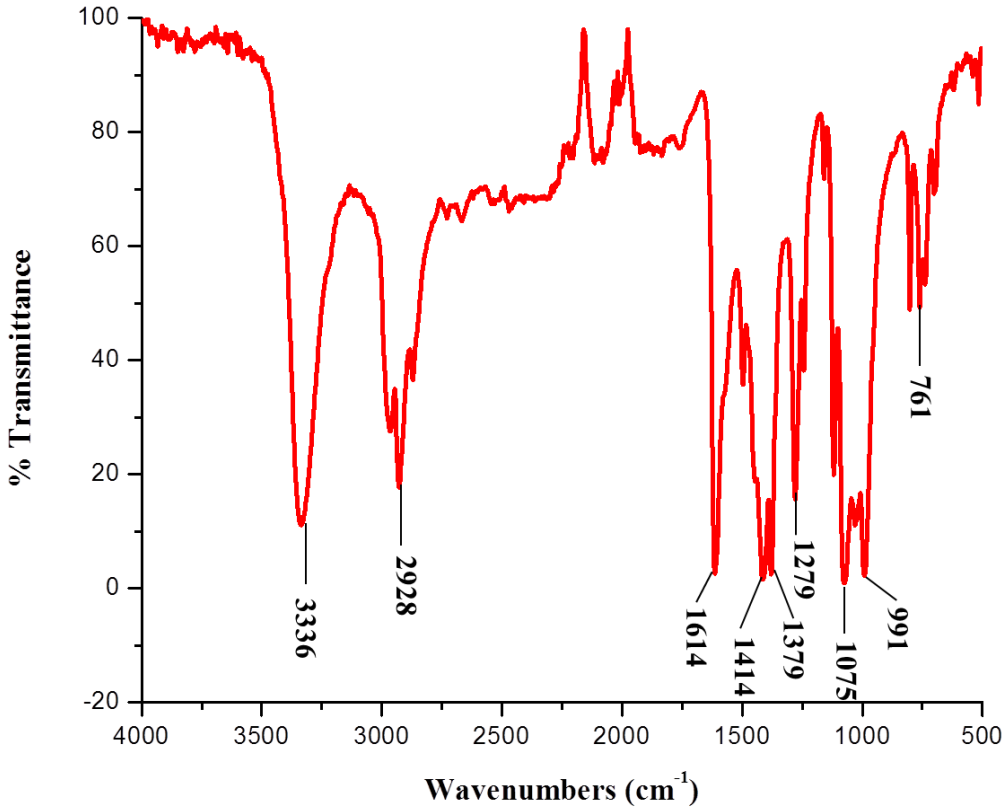

Fig. S53. IR (film) spectrum of **4[BF_4]**

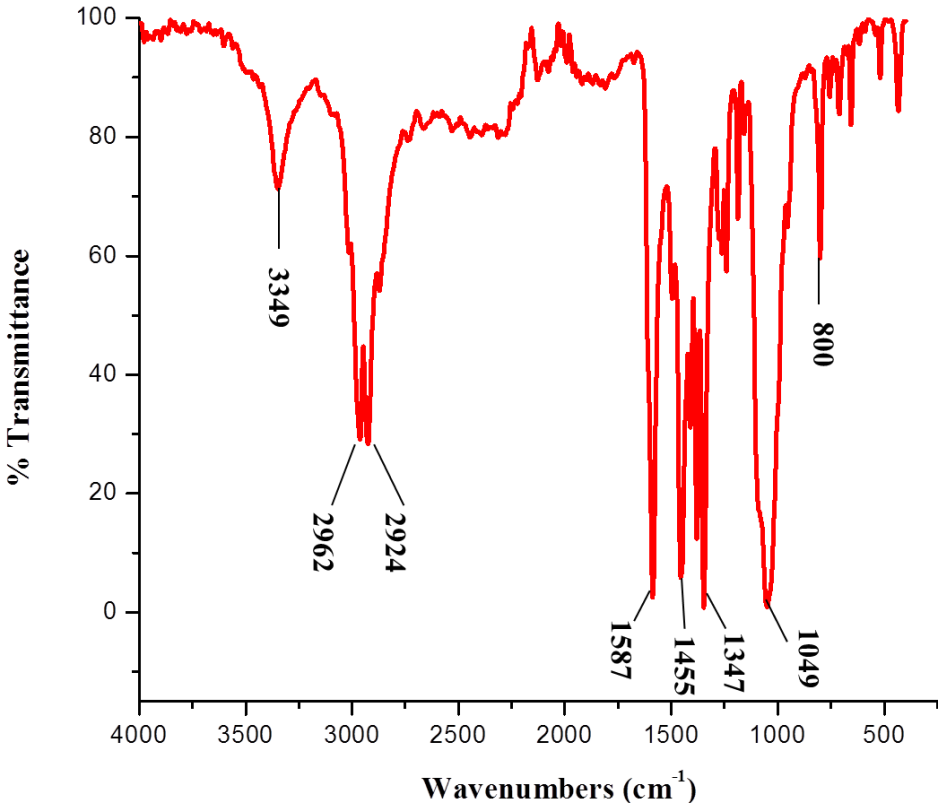

Fig. S54. IR (film) spectrum of **5a[PF_6]**

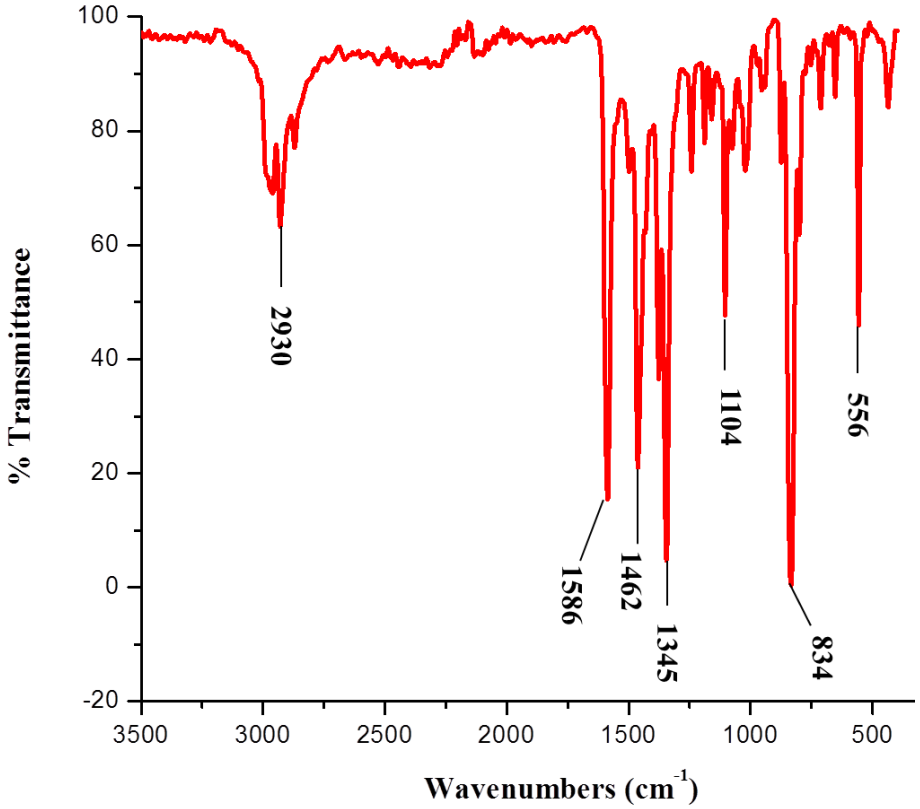

Fig. S55. IR (film) spectrum of **5b[PF_6]**

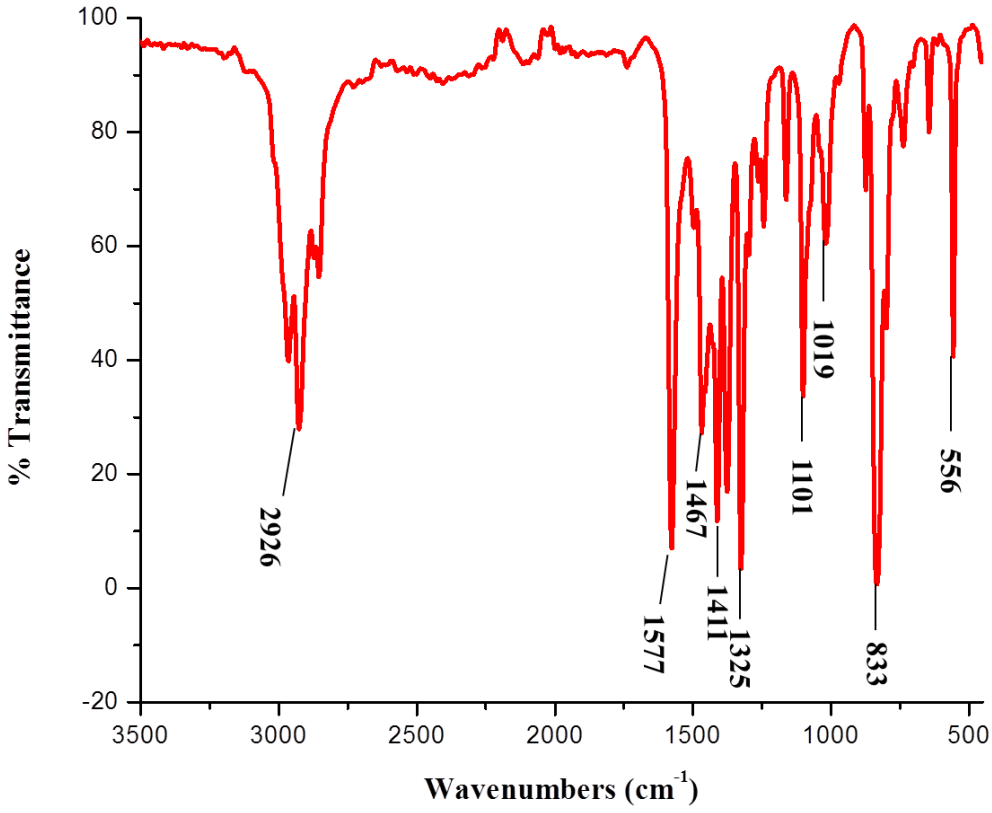

Fig. S56. IR (film) spectrum of **6a[PF_6]**

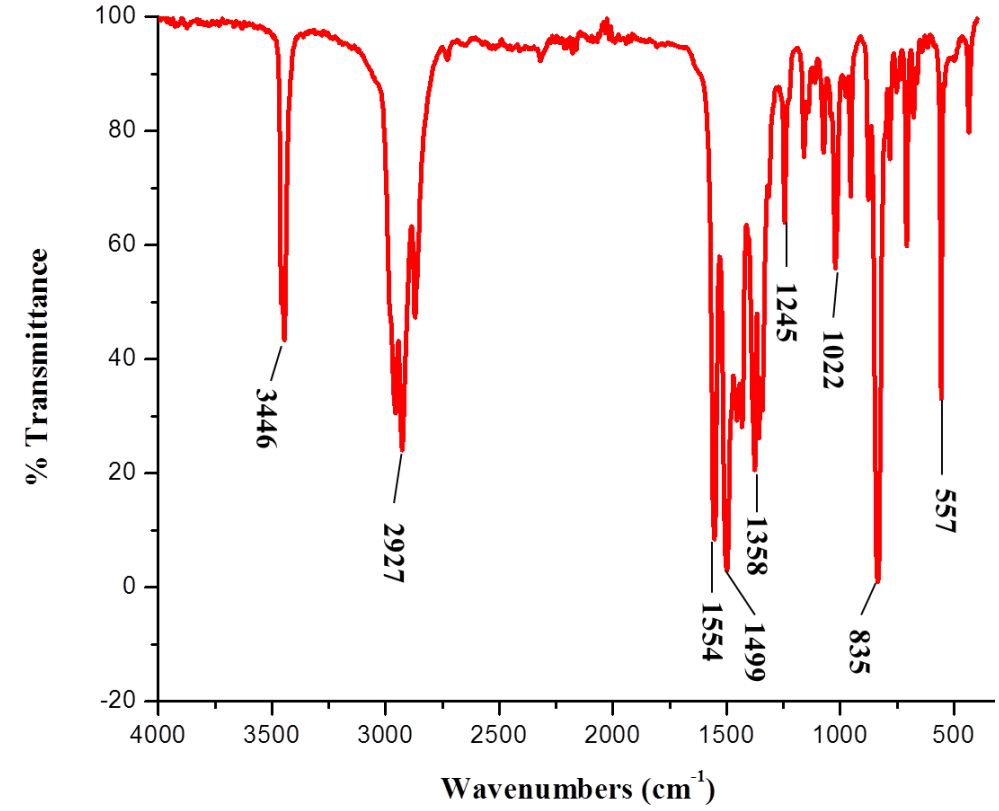

Fig. S57. IR (film) spectrum of **6b[PF_6]**

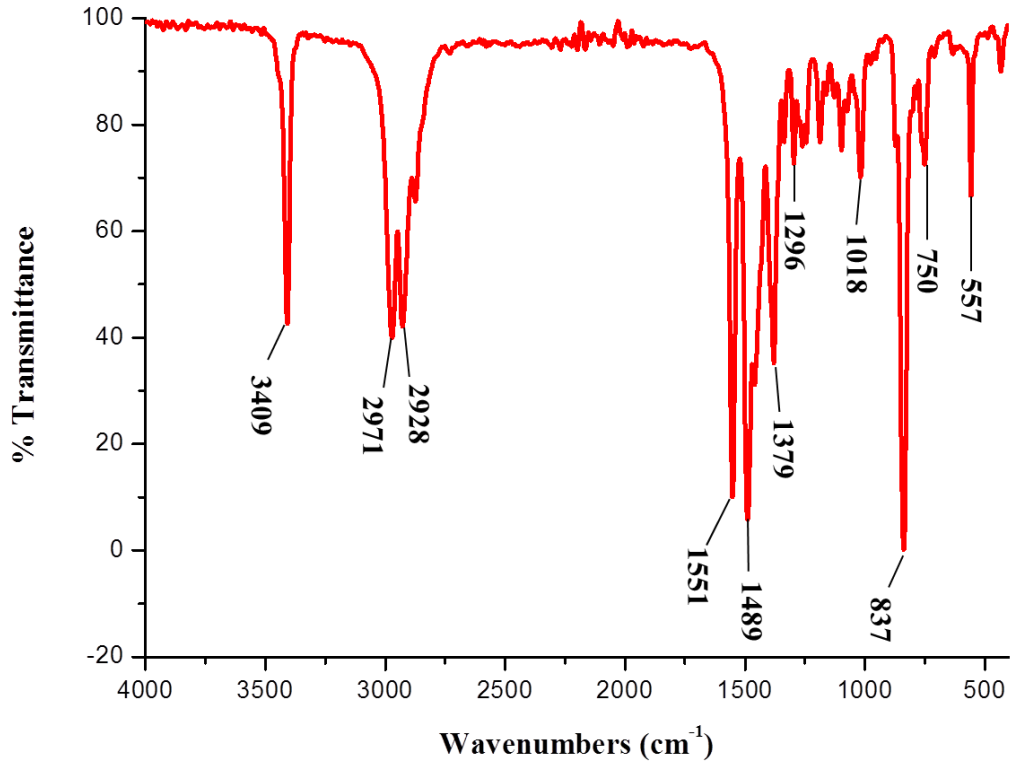

Fig. S58. IR (film) spectrum of **6c[PF_6]**

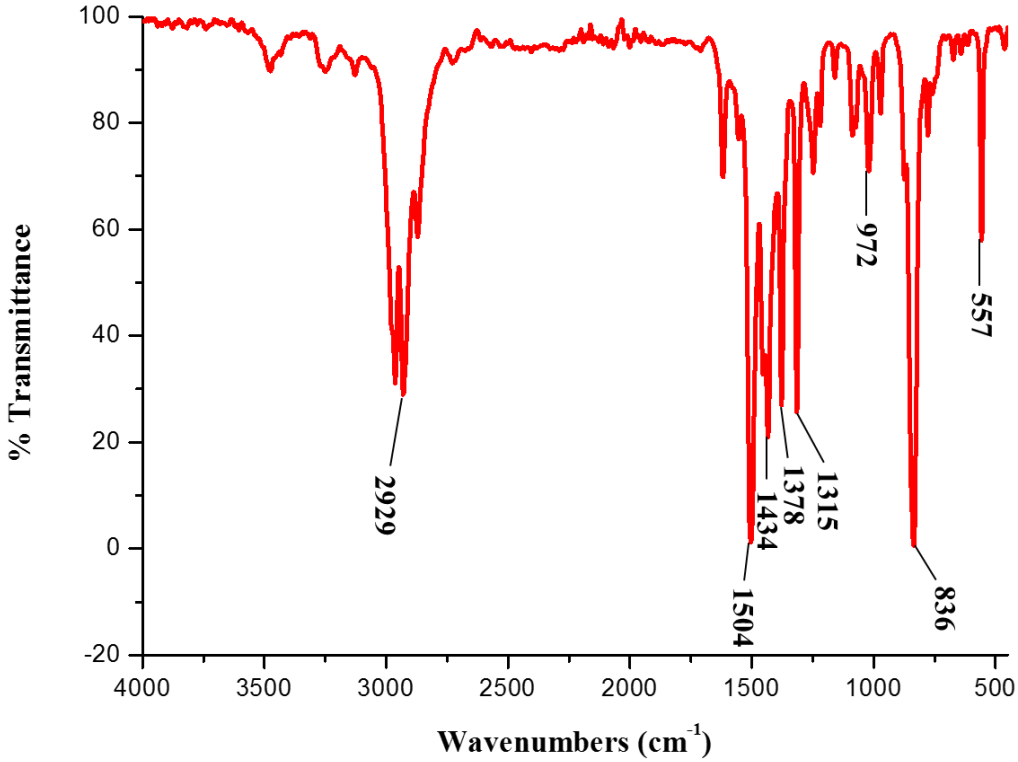

V. UV-Vis Spectra

Fig. S59. UV-Vis spectra of **1** and **2**

The red line corresponds to **1** and the black line corresponds to **2**.